scientific reports

Check for updates

OPEN

Scalable distributed gate-model quantum computers

Laszlo Gyongyosi[1,2]✉ & Sandor Imre[1]

A scalable model for a distributed quantum computation is a challenging problem due to the complexity of the problem space provided by the diversity of possible quantum systems, from small-scale quantum devices to large-scale quantum computers. Here, we define a model of scalable distributed gate-model quantum computation in near-term quantum systems of the NISQ (noisy intermediate scale quantum) technology era. We prove that the proposed architecture can maximize an objective function of a computational problem in a distributed manner. We study the impacts of decoherence on distributed objective function evaluation.

As the development of quantum computers evolve extensively[1–29], the power of quantum computations has become more interpretable for efficient problem-solving. However, while experimental quantum computers are currently under development, smaller quantum devices and quantum terminals are currently available in practice. As an adequate answer to the quantum supremacy of quantum computers, the development of the quantum Internet[30–43] has already started both in theory and experiment[32,34,36,39,44–46], with a primary aim to provide unconditional security with advanced network services[31–34,36,38,41,44–64]. A common attribute of quantum computer architectures and the quantum Internet[30,31,52,65–119], from an abstract theoretical point of view, are scalable distributed quantum systems[120–137]. Performing quantum computation in a distributed quantum system can also be approached as a maximization problem since a computational problem fed into the quantum system defines an objective function. The optimization of a distributed problem solving is therefore equivalent to a maximization of the objective function of a computational problem fed into the distributed quantum system (Objective function examples can be found in[5,8,9].). A primary aim of these distributed quantum systems is therefore the maximization of an objective function in a distributed manner, via quantum CPUs in a quantum computer[1–4,14,138–141]), or by quantum terminals[39,40,45,64,125,126,128,131,133] in a quantum Internet setting.

The problem of scalable quantum computation in a distributed quantum system is a challenge because of the complexity of the problem space provided by the diversity of possible quantum systems. The distributed quantum computational model has to include arbitrarily scaled quantum systems, from smaller quantum devices to large-scale quantum computers and the quantum Internet. As a corollary, the definition and parameterization of a scalable model for a distributed gate-model quantum computation is a hard problem, and no general solution is currently available.

Here, we study the problem of scalable quantum processing in distributed near-term quantum systems. We define a scalable distributed model of gate-model quantum computation and conceive the scaling attributes and unitaries of a distributed quantum information processing for problem-solving. The proposed scalable distributed quantum network integrates distributed quantum processing in arbitrarily scaled quantum systems.

In our context, an arbitrarily scaled quantum system can identify small, medium, or large-scale distributed quantum systems. The system model consists of an arbitrary number of quantum nodes connected by different levels of entangled connections (level of entanglement refers to the number of spanned nodes between a source and target node). The quantum system can refer to a quantum device, a quantum computer, or an arbitrary quantum Internet setting in which several quantum computers (quantum nodes) share entanglement to perform distributed quantum computations. The quantum nodes have to achieve the objective function maximization in a distributed way such that each node is allowed to apply local unitaries and connected via an arbitrary level of entanglement. In a small-scale system, the quantum nodes are connected by one-level entanglement while for a medium- or large-scale system, the level of entanglement between quantum nodes can be arbitrarily large. The local unitaries of the nodes are defined in a way that allows the distributed quantum system to implement a gate-model quantum computation in a distributed way.

We characterize a system model of a scalable distributed quantum system that allows for the performance of distributed gate-model quantum computation in a scalable manner. We define the scalable attributes of the system model and the gate parameters of the local unitaries of the quantum nodes for the objective function

[1]Department of Networked Systems and Services, Budapest University of Technology and Economics, Budapest 1117, Hungary. [2]MTA-BME Information Systems Research Group, Hungarian Academy of Sciences, Budapest 1051, Hungary. ✉email: gyongyosi@hit.bme.hu

maximization, assuming that multipartite entanglement is utilized in the local nodes, and evaluate a cost function. The system model also assumes that the distributed quantum network evolves with time; thus, we utilize the impacts of decoherence in the distributed objective function evaluation and maximization.

Since the proposed system model is parameterizable for different physical systems, the results are applicable for distributed quantum computations in quantum computers, quantum devices, quantum networking, and the quantum Internet. Derivations focus on near-term quantum systems such as qubit-based implementations, qubit-based quantum computer architectures, and entangled network structures connected by multipartite qubit entanglement; however, the results are extendable for arbitrary dimensional quantum systems.

The novel contributions of our manuscript are as follows:

- We define a distributed quantum system to implement a scalable distributed gate-model quantum computation.
- We conceive the unitary operations of the distributed system and prove that the distributed quantum system can maximize the objective function of an arbitrary computational problem.
- We reveal the impacts of decoherence on the distributed objective function evaluation and define a suitable cost function for scalable distributed quantum computation.

This paper is organized as follows. In Sect. 2, the problem statement and system model are given. Section 3 defines the distributed quantum computational model. In Sect. 4, the scaling methods are concealed. Finally, Sect. 5 concludes the results. Supplemental information is included in the Appendix.

Scalable distributed quantum system

Problem statement. The issues that need to be addressed are given in Problems 1–4.

Problem 1 *Define the scaling attributes of an arbitrary distributed quantum system to resolve an arbitrary computational problem in a distributed manner.*

Problem 2 *Define the unitary operations of the distributed system that allows for the implementation of a distributed gate-model quantum computation.*

Problem 3 *Prove that the distributed quantum system can maximize the objective function of an arbitrary computational problem fed into the distributed quantum system.*

Problem 4 *Determine the impacts of decoherence on the distributed objective function evaluation, and define a suitable cost function for the distributed quantum computation.*

The resolutions to Problems 1–4 are proposed in the Theorems and Lemmas of the manuscript.

System model. The system model of the N scalable distributed physical system is as follows. In $N = (V, S)$, the $|V|$ quantum nodes are connected via $|S|$, l-level entangled connections (An entangled connection between the quantum nodes refers to a shared multipartite entanglement. Between two nodes, x and y, the entangled connection identifies a bipartite quantum entanglement. For a qubit setting, the $d = 2$ dimensional twopartite maximally entangled states are the so-called Bell states; here one can assume the use of the $|\beta_{00}\rangle$ state, $|\beta_{00}\rangle = \frac{1}{\sqrt{2}}(|00\rangle + |11\rangle)$ in the system model.), where V is a set of quantum nodes and S is a set of entangled connections. For an l-level entangled connection, the $d(x,y)_{\mathrm{L}_l}$ hop distance in N is

$$d(x,y)_{\mathrm{L}_l} = 2^{l-1}, \tag{1}$$

with $d(x,y)_{\mathrm{L}_l} - 1$ intermediate nodes (The level l of an entangled connection assumes that each entanglement level doubles the hop-distance between x and y, which is a general model in quantum networking. It is also used in the so-called doubling architecture of entanglement distribution, in which the entanglement levels are increased via entanglement swapping[39,41]. Note, that l can model any hop-distance between the nodes.) between the nodes x and y. Thus, $l = 1$ refers to a direct connection between two quantum nodes x and y without intermediate quantum nodes in the distributed system N.

Proposition 1 *(Distributed quantum system for a scalable distributed gate-model quantum computation). An arbitrary distributed quantum system N is scalable via the entanglement level of entangled connections, by the gate parameters of the local unitaries of the quantum nodes, and by local measurements in the nodes. The N distributed quantum system can implement a scalable gate-model quantum computation in a distributed manner.*

Proof The level l of the entangled connections between the nodes depends on the physical size and topology of N. Without loss of generality, for an s small-scale distributed quantum system (quantum device, quantum terminal, smaller quantum computer),

$$l = 1, \tag{2}$$

while for an m medium, or l large-scale distributed quantum system (medium or large-scale quantum computer, quantum repeater network, arbitrary quantum communication network, quantum Internet),

$$l \geq 1. \tag{3}$$

A $\mathcal{P}(A \rightarrow B)$ computational path of N is modeled as a set $V = \{V_1, \ldots, V_L\}$ of L quantum nodes, with a set $S = \{E_1, \ldots, E_{L-1}\}$ of $L-1$ entangled connections between the nodes, where E_j identifies an entangled connection between d-dimensional quantum states j and k in nodes V_x and V_y. Focusing on near-term distributed quantum systems, we use $d = 2$; thus, j and k refer to qubits throughout the manuscript. The aim of the $\mathcal{P}(A \rightarrow B)$ computational path is to maximize a particular objective function $C_{\mathcal{P}(A \rightarrow B)}$ of an arbitrary computational problem in a distributed manner using the nodes and entangled connections of the path.

The allowed operations for a node pair $V_{xy} = \{V_x, V_y\}$ with a shared l-level entangled connection E_j, $j = 1, \ldots, L-1$ are defined as follows.

A scalable gate-model quantum computation can be set up in N by allowing the local nodes to perform local unitaries using the Pauli σ_x and σ_z operators. The local unitaries scaled by the gate parameters, in the following manner.

A node pair $\{V_x, V_y\}$ is allowed perform a local single-qubit unitaries[12,14]

$$U(X_j, \beta_j) = \exp\left(-i\beta_j X_j\right), \tag{4}$$

where $\beta_j \in [0, \pi]$ is the gate parameter of the unitary, while X is the Pauli σ_x operator, and

$$U(X_k, \beta_k) = \exp\left(-i\beta_k X_k\right), \tag{5}$$

on qubits j and k in nodes V_x and V_y, $\beta_k \in [0, \pi]$.

The node pair is also allowed to realize a distributed unitary

$$U(Z_jZ_k, \gamma_{jk}) = U(Z_jZ_k, \gamma_j)\, U(Z_jZ_k, \gamma_k) = \exp\left(-i(\gamma_j)Z_jZ_k\right) \exp\left(-i(\gamma_k)Z_jZ_k\right) \tag{6}$$

on qubits j and k using the l-level entangled connection $E_j = \langle jk \rangle$, where $\gamma_{jk} \in [0, 2\pi]$ is the gate parameter of the distributed unitary[12,14], defined as

$$\gamma_{jk} = \gamma_j + \gamma_k, \tag{7}$$

where $\gamma_j, \gamma_k \in [0, \pi]$ are the local gate parameters applied on qubits j and k, Z is the Pauli σ_z operator, while

$$\begin{aligned}
&U(Z_jZ_k, \gamma_{jk}) \\
&= U(Z_jZ_k, \gamma_j)\, U(Z_jZ_k, \gamma_k) \\
&= \exp\left(-i(\gamma_j)Z_jZ_k\right) \exp\left(-i(\gamma_k)Z_jZ_k\right) \\
&= \left(\cos(\gamma_j)I - i\sin(\gamma_j)Z_jZ_k\right)\left(\cos(\gamma_k)I - i\sin(\gamma_k)Z_jZ_k\right) \\
&= \cos(\gamma_j)\cos(\gamma_k)I - i\cos(\gamma_j)\sin(\gamma_k)Z_jZ_k - i\cos(\gamma_k)\sin(\gamma_j)Z_jZ_k - \sin(\gamma_j)\sin(\gamma_k)Z_jZ_kZ_jZ_k \\
&= \tfrac{1}{2}\left(\cos(\gamma_j - \gamma_k) + \cos(\gamma_j + \gamma_k)\right)I - i\left(\tfrac{1}{2}\left(\sin(\gamma_j + \gamma_k) - \sin(\gamma_j - \gamma_k)\right)\right)Z_jZ_k \\
&\quad - i\left(\tfrac{1}{2}\left(\sin(\gamma_j + \gamma_k) - \sin(\gamma_k - \gamma_j)\right)\right)Z_jZ_k - \tfrac{1}{2}\left(\cos(\gamma_j - \gamma_k) - \cos(\gamma_j + \gamma_k)\right)I \\
&= \cos(\gamma_j + \gamma_k)I - 2i\left(\tfrac{1}{2}\left(\sin(\gamma_j + \gamma_k) - \sin(\gamma_k - \gamma_j)\right)\right)Z_jZ_k.
\end{aligned} \tag{8}$$

Thus, setting

$$\gamma_j = \gamma_k = \tfrac{1}{2}\gamma_{jk}, \tag{9}$$

the result in (8) can be evaluated as

$$\begin{aligned}
U(Z_jZ_k, \gamma_{jk}) &= U(Z_jZ_k, \gamma_j)\, U(Z_jZ_k, \gamma_k) \\
&= \cos(\gamma_{jk})I - i\sin\left(\gamma'_{jk}\right)Z_jZ_k \\
&= \exp\left(-i(\gamma_{jk})Z_jZ_k\right).
\end{aligned} \tag{10}$$

A node V_x can also apply an U_x^C local coupling unitary to connect qubits i and j from entangled connections $\langle (i-1)(i) \rangle$ and $\langle jk \rangle$ in V_x, as

$$U_x^C = \exp\left(-itH^{(i,j)}\right) \tag{11}$$

where $H^{(i,j)}$ is a Hamiltonian, and also in V_y on the qubits k and $k+1$ of entangled connections $\langle jk \rangle$ and $\langle (k+1)(k+2) \rangle$, as

$$U_y^C = \exp\left(-itH^{(k,k+1)}\right) \tag{12}$$

where $H^{(k,k+1)}$ is a Hamiltonian, to connect qubits k and $k+1$, and remote entangled connections.

Therefore, the U_{xy} unitary associated to a given node pair $\{V_x, V_y\}$ connected by an l-level entanglement E_j in the distributed quantum system N is defined as

$$\begin{aligned} U_{xy} &= U_x U_y \\ &= U(B_j,\beta_j)U(Z_jZ_k,\gamma_j)U(B_k,\beta_k)U(Z_jZ_k,\gamma_k) \\ &= U(X_j,\beta_j)U(X_k,\beta_k)U(Z_jZ_k,\gamma_{jk})U_x^C U_y^C \\ &= \exp(-i\beta_j X_j)\exp(-i\beta_k X_k)\exp(-i\gamma_{jk}Z_jZ_k)\exp\left(-itH^{(i,j)}\right)\exp\left(-itH^{(k,k+1)}\right), \end{aligned} \tag{13}$$

where U_x is the unitary of a node V_x, $x = 1,\ldots,L$, defined as

$$U_x = U(X_j,\beta_j)U(Z_jZ_k,\gamma_j), \tag{14}$$

while U_y is the unitary of its neighbor node V_y, as

$$U_y = U(X_k,\beta_k)U(Z_jZ_k,\gamma_k). \tag{15}$$

Since unitaries (14) and (15) allows us to realize a gate-model quantum computation[14,29], it follows that the $\{V_x, V_y\}$ node pairs of the distributed quantum system N can implement quantum computation using their entangled connections in a distributed manner. □

Methods. **Proposition 2** *To model multipartite entanglement in a particular node V_x, qubit j has entangled connection with k to formulate $\langle jk\rangle$, and also with Γ_j remote qubits, $n_1,\ldots,n_{\Gamma_j}$, which are not neighbors of qubit k (These Γ_j qubits have no connections with qubit k.). The total number of qubits that are neighbor of j but not neighbor of k is $\Gamma_j + 1$.*

Proof Each entangled connection E_j has a contribution ζ_{E_j} to an $F_{\mathcal{P}(A\to B)}$ target function of a computational path $\mathcal{P}(A\to B)$ (will be proven in Sect. 3)

$$\begin{aligned} F_{\mathcal{P}(A\to B)} &= \max_{\forall\theta} \langle\varphi^*| C_{\mathcal{P}(A\to B)} |\varphi^*\rangle \\ &= \tfrac{1}{2}\sum_{j=1}^{L-1} \zeta_{E_j}, \end{aligned} \tag{16}$$

where $|\varphi^*\rangle$ is the output state of $\mathcal{P}(A\to B)$, defined as

$$|\varphi^*\rangle = U_{\mathcal{P}(A\to B)}|+\rangle, \tag{17}$$

where $|+\rangle = \frac{1}{\sqrt{2}}(|0\rangle + |1\rangle)$, while $U_{\mathcal{P}(A\to B)}$ is defined as a unitary sequence associated to $\mathcal{P}(A\to B)$, as

$$\begin{aligned} U_{\mathcal{P}(A\to B)} =& U_L U_{L-1}\ldots U_1 \\ =& U(X_L,\beta_L)U(X_{L-1},\beta_{L-1})U(Z_{L-1}Z_L,\gamma_{L-1,L})U(Z_{L-1}Z_{L-2},\gamma_{L-1,L-2}) \\ & \ldots U(X_2,\beta_2)U(X_1,\beta_1)U(Z_1Z_2,\gamma_{12}) \\ =& \prod_{j\in\mathcal{P}(A\to B)} U(X_j,\beta_j) \prod_{\langle jk\rangle\in\mathcal{P}(A\to B)} U(Z_jZ_k,\gamma_{jk}), \end{aligned} \tag{18}$$

where $\langle jk\rangle \in \mathcal{P}(A\to B)$ refers to an E_j entangled connection between qubits j and k on the computational path $\mathcal{P}(A\to B)$.

The n-qubit length input system $|s\rangle$ of the distributed system N, is defined as a product of σ_x eigenstates[12,14], as

$$|s\rangle = |+\rangle_1|+\rangle_2\ldots|+\rangle_n = |+\rangle^{\otimes n} = \tfrac{1}{\sqrt{2^n}}\sum_z |z\rangle, \tag{19}$$

where $|z\rangle$ is a computational basis state, z is an n-length string,

$$z = z_1 z_2 \ldots z_n, \tag{20}$$

where z_i identifies an i-th bit, $z_i \in \{-1, 1\}$, and $|+\rangle_i$ is the input system of an i-th computational path (As N is a quantum computer system or a quantum device with quantum registers, then $|s\rangle$ refers to a quantum register in the superposition of n qubits, while a given node A_i identifies the i-th source qubit, $|+\rangle_i$, of the n-length quantum register. In the current system model, the input system fed into the distributed system can also refer to a quantum register, physically not distributed between distant parties.) $\mathcal{P}(A_i\to B_i)$.

The nodes of the distributed system also can perform $M[m_b]$ local measurements in a base $m_b \in \{m_0, m_1\}$ (see (35), (36)) to realize an $\mathcal{L}_U$ upload[76,142] and an $\mathcal{L}_D$ download[76,143] procedure. The $\mathcal{L}_U$ upload procedure is an information delocalization method[76,142], in which a source system is uploaded by a source node onto the network state formulated by the entangled connections of the intermediate nodes of the distributed system. The $\mathcal{L}_D$ download procedure is an information localization procedure[76,143], in which the uploaded and transformed information (transformed by the local unitaries of the quantum nodes in our setting) is localized into a particular target node from the network state of intermediate nodes. Since the distributed quantum system evolves with

time, the timing of a local measurement also represents a scalable attribute in the distributed system (see (27) and (37)). □

Proposition 3 *In a source node A_i, the $\mathcal{L}_U(|+\rangle_i)$ uploading is realized by a $\mathcal{M}_B$ Bell measurement[76] applied on input system $|+\rangle_i$ and the first particle of chain $|\Phi\rangle_i$ that identifies the $|\Phi\rangle_i$ network state of computational path $\mathcal{P}(A_i \rightarrow B_i)$.*

Proof The $|\Phi\rangle_i$ network state is defined as

$$|\Phi\rangle_i = U(\vec{\theta}_i)\frac{1}{\sqrt{2}}\left(|0\rangle_{aux}(|0\rangle)_2^{2(L-1)} + |1\rangle_{aux}(|1\rangle)_2^{2(L-1)}\right), \tag{21}$$

where sub-index 1 identifies the first particle of $|\Phi\rangle_i$ of $\mathcal{P}(A_i \rightarrow B_i)$ maximally entangled with the remaining $2(L-1)$ qubits of the chain of $\mathcal{P}(A_i \rightarrow B_i)$.

The $\mathcal{L}_U(|+\rangle_i)$ uploading process results in

$$\begin{aligned}\mathcal{L}_U(\alpha_i|0\rangle + \beta_i|1\rangle) &= U\left(\vec{\theta}_i\right)\left(\alpha_i(|0\rangle)_2^{2(L-1)} + \beta_i(|1\rangle)_2^{2(L-1)}\right)\\ &= U\left(\vec{\theta}_i\right)\frac{1}{\sqrt{2}}\left((|0\rangle)_2^{2(L-1)} + (|1\rangle)_2^{2(L-1)}\right),\end{aligned} \tag{22}$$

where $\alpha_i|0\rangle + \beta_i|1\rangle = \frac{1}{\sqrt{2}}(|0\rangle + |1\rangle) = |+\rangle_i$.

Applying $\mathcal{L}_U(|+\rangle_i)$ for $i = 1, \ldots, n$, uploads the input system $|s\rangle$ in a distributed manner, as

$$\mathcal{L}_U(|s\rangle) = \mathcal{L}_U(|+\rangle_1|+\rangle_2 \ldots |+\rangle_n), \tag{23}$$

to the $|\Phi\rangle_1^n$ distributed network state formulated via n computational paths $\mathcal{P}(A_1 \rightarrow B_1), \ldots, \mathcal{P}(A_n \rightarrow B_n)$, as

$$\begin{aligned}|\Phi\rangle_1^n &= U(N)\frac{1}{\sqrt{2}}\left((|00\rangle)_1^{n2(L-1)} + (|11\rangle)_1^{n2(L-1)}\right)\\ &= U(N)\frac{1}{\sqrt{2}}\left(|0\rangle_1^n(|0\rangle)_{n+1}^{n2(L-1)} + |1\rangle_1^n(|1\rangle)_{n+1}^{n2(L-1)}\right),\end{aligned} \tag{24}$$

while indices $1, \ldots, n$ identify the auxiliary systems used for the uploading procedure in the n source nodes[76,142], while $U(N)$ the unitary of N is defined as,

$$U(N) = \prod_{j\in N} U(X_j, \beta_j) \prod_{\langle jk\rangle \in N} U(Z_jZ_k, \gamma_{jk}) = U\left(\vec{\theta}_n\right)U\left(\vec{\theta}_{n-1}\right)\ldots U\left(\vec{\theta}_1\right),$$

where $U(\vec{\theta}_i)$ refer to the unitary associated to an i-th path $\mathcal{P}(A_i \rightarrow B_i), i = 1, \ldots, n$, defined as a unitary sequence of L unitaries,

$$U\left(\vec{\theta}_i\right) = U_{i,L}U_{i,L-1}\ldots U_{i,1}, \tag{25}$$

where $U_{i,x}$ identifies the unitary of a given node V_x of $\mathcal{P}(A_i \rightarrow B_i)$, as

$$U_{i,1} = U\left(\beta_{i,1}, X_{i,1}\right)U\left(\gamma_{i,1}, Z_{i,1}\right), \tag{26}$$

and $U(\vec{\theta}_i)$ is a unitary sequence of $2L$ unitaries implemented via L nodes V_x, $x = 1, \ldots, L$, in $\mathcal{P}(A_i \rightarrow B_i)$.

The $\mathcal{L}_U(|s\rangle)$ operation therefore results in

$$\mathcal{L}_U(|s\rangle) = U(N)\frac{1}{\sqrt{2^n}}\left((|0\rangle)_{n+1}^{n2(L-1)} + (|1\rangle)_{n+1}^{n2(L-1)}\right), \tag{27}$$

that yields the output system of N

$$\left|\phi^*\right\rangle = U(N)|s\rangle \tag{28}$$

distributed between the n receiver nodes $B_1, \ldots, B_n$. Thus. the outputs of the n paths, $U(N)|s\rangle$ can be localized onto the n receivers in the downloading procedure[76,143].

To verify (22) and (27), we recall the formalisms of[144,145]. The input system $|+\rangle_i$ of a given node A_i can be rewritten as

$$|+\rangle_i = \lambda_0|0\rangle + \lambda_1|1\rangle, \tag{29}$$

and let $|\Phi\rangle_i$ be as given in (21), then

$$|\Phi\rangle_i|+\rangle_i = \sum_{k,s=0,1} \lambda_k U(\vec{\theta}_i)\frac{1}{\sqrt{2}}\left((M[m_s]|L\rangle)_2^{2(L-1)}\right)|m_s\rangle_1|k\rangle_0, \tag{30}$$

where indices 0 and 1 identify the input system $|+\rangle_i$ and the first qubit of the first EPR pair of chain $|\Phi\rangle_i$ that serves as an $|aux\rangle$ auxiliary qubit system, $\mathcal{H}_{aux} = \mathbb{C}^2$, maximally entangled with the $2(L-1)$-qubit length system

$(|L\rangle)_2^{2(L-1)}$, $\mathcal{H}_L = \mathbb{C}^{2^{\otimes 2(L-1)}}$, formulating orthogonal states as $(|L\rangle)_2^{2(L-1)} = \left\{|0\rangle_2^{2(L-1)}, |1\rangle_2^{2(L-1)}\right\}$, while $\{|m_s\rangle\}$ is an orthogonal basis[76,144,145].

Then, in node A_i an $\mathcal{M}_B$ Bell measurement is applied on subsystems 0 and 1, that yields a projection onto

$$\mathcal{M}_B(A_i) : |B_1\rangle_{10} = \sum_j \left|m_j\right\rangle_1 \left|j\right\rangle_0, \tag{31}$$

while the $\left|\Phi'\right\rangle_i$ post-measurement network state is evaluated as

$$\begin{aligned}\left|\Phi'\right\rangle_i &= \sum_j U\left(\vec{\theta}_i\right)\left(\lambda_j M\left[m_j\right](|L\rangle)_2^{2(L-1)}\right)\\ &= U\left(\vec{\theta}_i\right)\left(\lambda_0(|0\rangle)_2^{2(L-1)} + \lambda_0(|1\rangle)_2^{2(L-1)}\right)\\ &= U\left(\vec{\theta}_i\right)\tfrac{1}{\sqrt{2}}\left((|0\rangle)_2^{2(L-1)} + (|1\rangle)_2^{2(L-1)}\right)\\ &= \mathcal{L}_U\left(\tfrac{1}{\sqrt{2}}(|0\rangle + |1\rangle)\right),\end{aligned} \tag{32}$$

which coincidences with (22).

Extending the derivations to n computational paths such that the paths realize the n-qubit unitary $U(N)$, each A_i apply a Bell measurement $\mathcal{M}_B(A_i)$, thus the post-measurement network state $\left|\Phi'\right\rangle_1^n$ is as

$$\begin{aligned}\left|\Phi'\right\rangle_1^n &= U(N)\sum_{i,j}\left(\lambda_{i,j} M\left[m_{i,j}\right](|L\rangle)_{n+1}^{n2(L-1)}\right)\\ &= U(N)\left(\lambda_{1,0}\lambda_{2,0}\ldots\lambda_{n,0}(|0\rangle)_{n+1}^{n2(L-1)} + \lambda_{1,1}\lambda_{2,1}\ldots\lambda_{n,1}(|1\rangle)_{n+1}^{n2(L-1)}\right)\\ &= U(N)\left(\lambda_0^n(|0\rangle)_{n+1}^{n2(L-1)} + \lambda_1^n(|1\rangle)_{n+1}^{n2(L-1)}\right)\\ &= U(N)\tfrac{1}{\sqrt{2^n}}\left((|0\rangle)_{n+1}^{n2(L-1)} + (|1\rangle)_{n+1}^{n2(L-1)}\right)\\ &= \mathcal{L}_U(|+\rangle_1|+\rangle_2\ldots|+\rangle_n),\end{aligned} \tag{33}$$

where $(|L\rangle)_{n+1}^{n2(L-1)} = \left\{|0\rangle_{n+1}^{n2(L-1)}, |1\rangle_{n+1}^{n2(L-1)}\right\}$ defined on $\mathcal{H}_L = \mathbb{C}^{2^{\otimes n2(L-1)}}$ since the entangled network structure of the distributed system is formulated via $n2(L-1)$ entangled states over the n computational paths, while n auxiliary qubit systems, $|aux\rangle_1|aux\rangle_2\ldots|aux\rangle_n$, are measured via the Bell measurements in the n source nodes, $\mathcal{H}_{aux_{1\ldots n}} = \mathbb{C}^{2^{\otimes n}}$, that confirms the result in (27).

The $\mathcal{L}_D$ downloading process[76,143] for receiver node B_i results in

$$\mathcal{L}_D\left(U(\vec{\theta}_i)\tfrac{1}{\sqrt{2}}\left((|0\rangle)_2^{2(L-1)} + (|1\rangle)_2^{2(L-1)}\right)\right) = U(\vec{\theta}_i)|+\rangle_i. \tag{34}$$

To obtain (34) in B_i, $M[m_b]$ local measurements in a m_b suitable basis are applied on the remaining $2(L-1)-1$ qubits in the $L-1$ nodes of $\mathcal{P}(A_i \to B_i)$ between A_i and B_i. Recalling the formalisms of[144,145], for an i-th node, the $M[m_b]$ local measurement is set in bases $m_b \in \{m_0, m_1\}$, as

$$M[m_0] = |\psi_0\rangle\langle 0|, \tag{35}$$

and

$$M[m_1] = |\psi_1\rangle\langle 1|, \tag{36}$$

where $|\psi_0\rangle = \cos\frac{\varsigma}{2}|0\rangle + e^{i\alpha}\sin\frac{\varsigma}{2}|1\rangle$, $|\psi_1\rangle = \sin\frac{\varsigma}{2}|0\rangle - e^{i\alpha}\cos\frac{\varsigma}{2}|1\rangle$, with $\varsigma \in [0,\pi]$. (Assuming that the entangled connections between the nodes are maximally entangled, $\varsigma = \pi$, and $\varsigma < \pi$ otherwise. This parameter is also referred to as entanglement factor, see also[76]). Then, it can be verified[76,143] that by applying $M[m_b]$ local measurements in the $L-2$ intermediate nodes between A_i and B_i as defined by (35) and (36), Bob B_i obtains the result $U(\vec{\theta}_i)|+\rangle_i$ with probability $\Pr\left(U(\vec{\theta}_i)|+\rangle_i\right) = 1 - \cos\frac{\varsigma}{2}$.

Therefore, applying the measurement procedure in the intermediate nodes of the n computational paths, results in (28) at the receiver side in a distributed manner, as

$$\left|\phi^*\right\rangle = \mathcal{L}_D\left(U(N)\tfrac{1}{\sqrt{2^n}}\left((|0\rangle)_{n+1}^{n2(L-1)} + (|1\rangle)_{n+1}^{n2(L-1)}\right)\right), \tag{37}$$

with probability

$$\Pr\left(\left|\phi^*\right\rangle\right) = \prod_{i=1}^{n}\left(1 - \cos\tfrac{\varsigma_i}{2}\right) \tag{38}$$

over the n paths. Thus, if the network is maximally entangled it yields a deterministic download at the receiver with $\Pr(|\phi^*\rangle) = 1$.

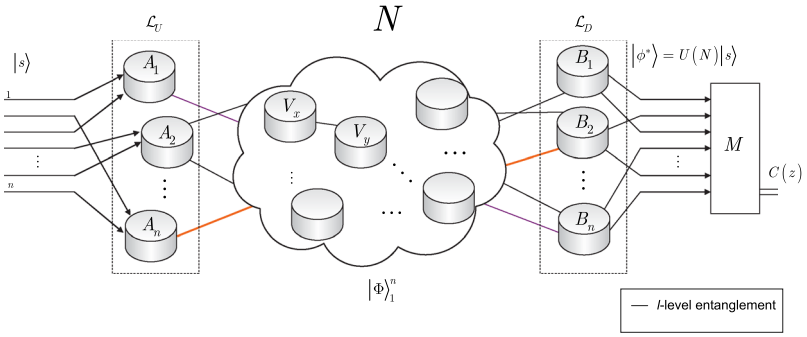

Figure 1. The schematic model of the distributed physical system N that realizes a scalable distributed quantum computation with arbitrary-level entangled connections. The $|s\rangle = |+\rangle_1 \ldots |+\rangle_n$ input system is distributed via n source nodes $A_1, \ldots, A_n$ through a chain of intermediate nodes via l-level entangled connections to the n receiver nodes $B_1, \ldots, B_n$, where $|+\rangle = \frac{1}{\sqrt{2}}(|0\rangle + |1\rangle), |s\rangle = \frac{1}{\sqrt{2^n}} \sum_z |z\rangle$, while $|z\rangle$ is an n-qubit length computational basis state. The aim of the distributed network system N is to maximize a C objective function of a computational problem in a distributed manner. The distributed system realizes the distributed unitary $U(N)$ and outputs a distributed system $|\phi^*\rangle = U(N)|s\rangle$. The M distributed measurements are performed in the n receiver nodes $B_1, \ldots, B_n$ to produce the string z that allows the nodes to evaluate $C(z)$ in a distributed way. The $|s\rangle$ input system is uploaded via the $\mathcal{L}_U(|s\rangle) = \mathcal{L}_U(|+\rangle_1 \ldots |+\rangle_n)$ distributed uploading process to the distributed network state $|\Phi\rangle_1^n = U(N)\frac{1}{\sqrt{2}}\left((|00\rangle)_1^{n2(L-1)} + (|11\rangle)_1^{n2(L-1)}\right) = U(N)\frac{1}{\sqrt{2}}\left(|0\rangle_1^n(|0\rangle)_{n+1}^{n2(L-1)} + |1\rangle_1^n(|1\rangle)_{n+1}^{n2(L-1)}\right)$, where $|\Phi\rangle_i = U\left(\vec{\theta}_i\right)\frac{1}{\sqrt{2}}\left(|0\rangle_1(|0\rangle)_2^{2(L-1)} + |1\rangle_1(|1\rangle)_2^{2(L-1)}\right)$, where index 1 identifies the first particle of computational path $\mathcal{P}(A_i \to B_i)$, formulated via the results of the unitaries of the n computational paths, where an i-th path $\mathcal{P}(A_i \to B_i), i = 1, \ldots, n$, realizes an $U\left(\vec{\theta}_i\right) = U_{i,L}U_{i,L-1}\ldots U_{i,1}$ unitary sequence of $2L$ unitaries in L nodes $V_x, x = 1, \ldots, L$, where $U_{i,1} = U\left(\beta_{i,1}, X_{i,1}\right)U\left(\gamma_{i,1}, Z_{i,1}\right)$. The $\mathcal{L}_U(|s\rangle) = \mathcal{L}_U(|+\rangle_1)\ldots\mathcal{L}_U(|+\rangle_n)$ uploading process is distributed among the n nodes, where $\mathcal{L}_U(|+\rangle_i)$ is realized in an i-th source node A_i as $\mathcal{L}_U(\alpha_i|0\rangle + \beta_i|1\rangle) = U\left(\vec{\theta}_i\right)\left(\alpha_i(|0\rangle)_2^{2(L-1)} + \beta_i(|1\rangle)_2^{2(L-1)}\right) = U\left(\vec{\theta}_i\right)\frac{1}{\sqrt{2}}\left((|0\rangle)_2^{2(L-1)} + (|1\rangle)_2^{2(L-1)}\right)$. The $\mathcal{L}_D$ downloading process results in $\mathcal{L}_D\left(U\left(\vec{\theta}_i\right)\frac{1}{\sqrt{2}}\left((|0\rangle)_2^{2(L-1)} + (|1\rangle)_2^{2(L-1)}\right)\right) = U\left(\vec{\theta}_i\right)|+\rangle_i$ for receiver node B_i. Applying $\mathcal{L}_U$ and $\mathcal{L}_D$ for all source and receiver nodes, results in $\mathcal{L}_D(\mathcal{L}_U(|+\rangle_1 \ldots |+\rangle_n)) = U(N)|s\rangle$ at the receiver in a distributed manner.

The proof is concluded here. □

The system model of the scalable distributed physical system N is depicted in Fig. 1.

The schematic model of a computational path $\mathcal{P}(A \to B)$ in a distributed physical system N is depicted in Fig. 2. (Local measurements of downloading procedure are not shown.)

Ethics statement. This work did not involve any active collection of human data.

Quantum processing in a distributed quantum system

Theorem 1 *An objective function C can be maximized in the distributed quantum system N via a target function $F = \sum_{\langle jk\rangle \in N} F_{\langle jk\rangle} = \max_{\forall\theta} \langle\phi^*|C|\phi^*\rangle$, where $\langle jk\rangle$ is an l-level, $l \geq 1$, entangled connection between qubits j and k.*

Proof Let N be the physical distributed quantum system, with a particular objective function C of a computational problem subject of a maximization. To simplify the discussion in the following section, allow us to focus on a single computational path $\mathcal{P}(A \to B)$, thus we set $n = 1$, and $N = \mathcal{P}(A \to B)$ with $|s\rangle = |+\rangle$; however, the derivations and results are not restricted to this case.

Let $U(\vec{\theta})$ be the unitary realized via the computational path $\mathcal{P}(A \to B)$, as

$$U\left(\vec{\theta}\right) = U_{2L}(\theta_{2L})U_{2L-1}(\theta_{2L-1})\cdots U_1(\theta_1), \tag{39}$$

where $i = 1, \ldots, 2L$, L is the number of nodes of N (number of distributed subsystems), $2L$ is the total number of unitaries in the L nodes (each node is defined via 2 unitaries) θ_i is a gate parameter associated with U_i, i.e., $\theta_i = \beta_i$ or $\theta_i = \gamma_i$, and $\vec{\theta}$ is the gate parameter vector defined as

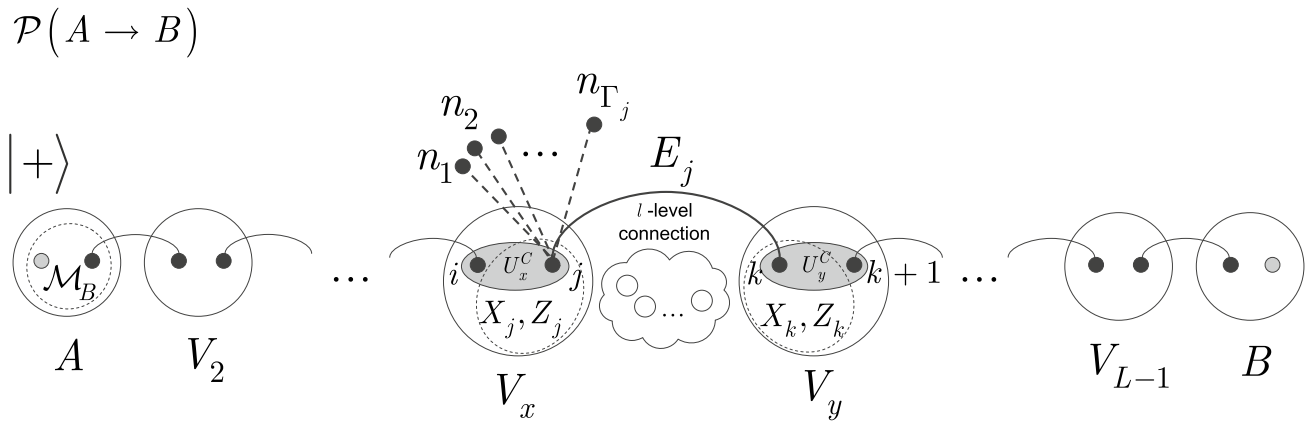

Figure 2. Evaluation of target function value F of a computational problem via a distributed computational path $\mathcal{P}(A \to B)$ between a distant source node A and receiver node B in a distributed system N with $L-2$ intermediate nodes $V_x, x = 2, \ldots, L-1$, with multipartite entanglement in the local nodes. Alice applies an $\mathcal{M}_B$ Bell measurement on the input system $|+\rangle$ and on the first particle of the chain to achieve the $\mathcal{L}_U(|+\rangle)$ uploading procedure. A node pair $V_{xy} = \{V_x, V_y\}$ with a shared l-level entangled connection E_j, $j = 1, \ldots, L-1$ ($l = 1$ for a small-scale system while $l \geq 1$ for a medium- and large-scale system by a convention) is allowed to (1) apply a local coupling unitary $U_x^C = \exp\left(-itH^{(i,j)}\right)$ and $U_y^C = \exp\left(-itH^{(k,k+1)}\right)$ to connect qubits i (connected to V_{x-1}) to and j in V_x, and qubits k and $k+1$ (connected to V_{x+1}), (2) to perform a local single-qubit unitaries $U\left(X_j, \beta_j\right)$ and $U(X_k, \beta_k)$ on qubits j and k in V_x and V_y, (3) to realize a distributed two-qubit unitary $U\left(Z_j Z_k, \gamma_{jk}\right)$ on qubits j and k using the l-level entangled connection E_j, and (4) to apply an $M[m_b]$ in basis $m_b \in \{m_0, m_1\}$, local measurement to realize the $\mathcal{L}_D$ download into B. In a given V_x, qubit j formulates a multipartite entanglement: j has an entangled connection with qubit k in V_y , and j is also entangled with Γ_j other neighbor qubits, $n_1, \ldots, n_{\Gamma_j}$, called remote entangled connections of j (not neighbors of qubit k), and the total number of qubits that are neighbors of j but not neighbors of k is $\Gamma_j + 1$. Each entangled connection E_j has a contribution ζ_{E_j} to the expected target function value $F_{\mathcal{P}(A \to B)} = \frac{1}{2}\sum_{j=1}^{L-1} \zeta_{E_j}$. (Operations associated with a particular qubit in a given node are depicted by dashed circles.)

$$\vec{\theta} = (\theta_1, \ldots, \theta_{2L-1}, \theta_{2L})^T. \tag{40}$$

Assuming that N consist of g single-qubit unitaries and m two-qubit unitaries for the entangled qubit pairs (m qubit pair connection in N), such that

$$L = g + m, \tag{41}$$

unitary $U(\vec{\theta})$ from (39) can be rewritten as

$$U\left(\vec{\theta}\right) = U\left(B, \vec{\beta}\right) U(C, \vec{\gamma}), \tag{42}$$

where

$$U\left(B, \vec{\beta}\right) = \prod_{j=1}^{g} U\left(B_j, \beta_j\right), \tag{43}$$

where $\vec{\beta}$ is the gate parameter vector,

$$\vec{\beta} = \left(\beta_1, \ldots, \beta_g\right)^T, \tag{44}$$

and

$$B = \sum_j B_j \tag{45}$$

where $B_j = X_j = \sigma_x^j$[12,14], and

$$U\left(B_j, \beta_j\right) = \exp\left(-i\beta_j X_j\right), \tag{46}$$

and $U(C, \vec{\gamma})$ is defined as[14]

$$U(C,\vec{\gamma}) = \prod_{\langle jk\rangle \in N} U\left(C_{jk},\gamma_{jk}\right), \tag{47}$$

where $\langle jk\rangle \in N$ is an l-level, $l \geq 1$, entangled connection between qubits j and k, with gate parameter vector

$$\vec{\gamma} = (\gamma_1,\ldots,\gamma_m)^T,$$

and

$$U\left(C_{jk},\gamma_{jk}\right) = U\left(Z_jZ_k,\gamma_{jk}C_{jk}\right) = \exp\left(-i\gamma_{jk}C_{jk}Z_jZ_k\right), \tag{48}$$

where $Z_jZ_k = \sigma_z^j\sigma_z^k$.

At a particular physical entangled connection topology in N, the objective function C can be written as

$$C(z) = \sum_{\langle jk\rangle \in N} C_{jk}(z), \tag{49}$$

where $C_{jk}(z)$ is the objective function component[12,14] evaluated for entangled connection $\langle jk\rangle \in N$, as

$$C_{jk}(z) = \tfrac{1}{2}\left(1 - z_jz_k\right), \tag{50}$$

where z is an n-length input bitstring,

$$z = z_1z_2\ldots z_n, \tag{51}$$

and z_i identifies an i-th bit, $z_i \in \{-1,1\}$.

For a given z, a $|z\rangle$ computational basis state is defined as

$$|z\rangle = |z_1z_2\ldots z_n\rangle \tag{52}$$

and $|\varphi\rangle$ output system of N at a single path at input (52) is defined as (For a level-p circuit, a set of p $\vec{\beta}$ and $\vec{\gamma}$ gate parameter vectors are used as $\vec{\beta}^{(1)},\ldots,\vec{\beta}^{(p)}$, and $\vec{\gamma}^{(1)},\ldots,\vec{\gamma}^{(p)}$. For simplicity, here we assume $p = 1$, however the results can be extended for arbitrary p[14]. For further details, see[14].)

$$\begin{aligned}
|\varphi\rangle &= U\left(\vec{\theta}\right)|z\rangle \\
&= U\left(B,\vec{\beta}\right)U(C,\vec{\gamma})|z\rangle \\
&= U\left(B,\vec{\beta}\right)\prod_{\langle jk\rangle \in N} U\left(C_{jk}(z),\gamma_{jk}\right)|z\rangle \\
&= \prod_j \exp\left(-i\beta_jX_j\right)\prod_{\langle jk\rangle \in N}\exp\left(-i\gamma_{jk}C_{jk}(z)Z_jZ_k\right)|z\rangle.
\end{aligned} \tag{53}$$

Then, let $|s\rangle$ be an n-qubit length input system of N, defined as in (19), thus for $n = 1$,

$$|s\rangle = |+\rangle, \tag{54}$$

and the output system $|\varphi^*\rangle$ is evaluated as given in (17).

The maximization of objective function C is identified via a target function F, as

$$\begin{aligned}
F &= \max_{\forall\theta}\left\langle \vec{\gamma},\vec{\beta},C|\,C|\vec{\gamma},\vec{\beta},C\right\rangle \\
&= \max_{\forall\theta}\left\langle \varphi^*|\,C|\varphi^*\right\rangle,
\end{aligned} \tag{55}$$

and for a particular entangled connection $\langle jk\rangle$ of N, the aim is the maximization of target function $F_{\langle jk\rangle}$, as

$$F_{\langle jk\rangle} = \max_{\forall\theta}\left(\left(-\tfrac{1}{2}\right)\left\langle \varphi^*_{N,jk}\middle|Z_jZ_k\middle|\varphi^*_{N,jk}\right\rangle\right), \tag{56}$$

where $\left|\varphi^*_{N,jk}\right\rangle$ is a target state defined as

$$\begin{aligned}
\left|\varphi^*_{N,jk}\right\rangle &= \left|\gamma_{jk},\beta_k,\beta_j,C_{jk}\right\rangle \\
&= U\left(B,\beta_j\right)U\left(B,\beta_k\right)U\left(C_{jk}(z),\gamma_{jk}\right)|s\rangle.
\end{aligned} \tag{57}$$

For the total system N, the objective function values of all entangled connections are summed, thus $C(z)$ is as given in (49).

For all connected qubits, the target function is set as

$$\begin{aligned} F &= \sum_{\langle jk\rangle \in N} F_{\langle jk\rangle} \\ &= \max_{\forall\theta} \left\langle \varphi^* \right| C \left| \varphi^* \right\rangle \\ &= \max_{\forall\langle jk\rangle \in N} \left(\left(-\tfrac{1}{2}\right) \sum_{\langle jk\rangle \in N} \left\langle \varphi^*_{N,jk} \right| C_{jk} \left| \varphi^*_{N,jk} \right\rangle \right) \\ &= \left(-\tfrac{1}{2}\right) \max_{\forall\langle jk\rangle \in N} \left(\sum_{\langle jk\rangle \in N} \left\langle \varphi^*_{N,jk} \right| Z_j Z_k \left| \varphi^*_{N,jk} \right\rangle \right), \end{aligned} \tag{58}$$

where $\left|\varphi^*_{N,jk}\right\rangle$ is given in (57).

Then, assuming that N consists of n computational paths, and $|s\rangle$ is an n-qubit length input as defined in (19), the result in (58) can be extended as

$$\begin{aligned} F &= \sum_{\langle jk\rangle \in N} F_{\langle jk\rangle} \\ &= \max_{\forall\theta} \left\langle \phi^* \right| C \left| \phi^* \right\rangle, \end{aligned} \tag{59}$$

that concludes the proof. □

Distributed computational system as an extended correlation space. **Lemma 1** (The distributed computational space is an extended correlation space). *The $\mathcal{D}(N)$ distributed computational space of N is an extended correlation space with n entangled computational paths, $\mathcal{P}(A_i \rightarrow B_i), i = 1, \ldots, n$ between n source and receiver nodes.*

Proof Using the correlation space (The correlation space is an abstract mathematical model of a physical system defined via a matrix product state (MPS) representation and open-boundary conditions[76,144,145].) formalism[144,145], we first rewrite $|\varphi^*\rangle$ from (17), as

$$\left|\varphi^*\right\rangle = \sum_{x_1,\ldots,x_L} \langle B|M[x_L]M[x_{L-1}]\ldots M[x]|A\rangle |x_1,\ldots,x_L\rangle, \tag{60}$$

where $x_i \in \{0,1\}, i = 1,\ldots,L$, $M[x_i]$ is a 2×2 matrix, $|x_i\rangle$ is a local state vector associated to node V_i, as

$$|x_i\rangle = c_0^{(i)}|0\rangle + c_1^{(i)}|1\rangle, \tag{61}$$

and $M[x_i]$ is defined as

$$M[x_i] = \bar{c}_0^{(i)} M[0] + \bar{c}_1^{(i)} M[1], \tag{62}$$

with relation[76,144,145]

$$(\langle x_1| \otimes \ldots \otimes \langle x_L|)|\psi_L\rangle = \langle x_L|M[x_{L-1}]\ldots M[x_1]|+\rangle, \tag{63}$$

where $|+\rangle = \frac{1}{\sqrt{2}}(|0\rangle + |1\rangle)$, while $|A\rangle$ and $|B\rangle$ are $d = 2$ dimensional vectors that represent the input and output systems (boundary conditions in the extended correlation space).

The system state of (60) can be rewritten as

$$\left|\varphi^*\right\rangle = \sum_{x_1,\ldots,x_L} \langle x_L|M[x_{L-1}]\ldots M[x_1]|+\rangle |x_1,\ldots,x_L\rangle. \tag{64}$$

By recalling Observation 2 from[145], allows us to the define δ_i via the $\varsigma \in [0,\pi]$ measurement coefficient used in the definition of measurement operators (35) and (36), as

$$\delta_i = \arg\left(\sin(\omega_i) + \cos(\omega_i)\exp\left(i\tfrac{\varsigma}{2}\right)\right), \tag{65}$$

where ω_i identifies computational bases $\left|b_{\omega_i}\right\rangle \in \left\{\left|0_{\omega_i}\right\rangle, \left|1_{\omega_i}\right\rangle\right\}$, as

$$\left|b_{\omega_i}\right\rangle = \begin{cases} \left|0_{\omega_i}\right\rangle = \sin(\omega_i)|0\rangle + \cos(\omega_i)|1\rangle \\ \left|1_{\omega_i}\right\rangle = \cos(\omega_i)|0\rangle - \sin(\omega_i)|1\rangle \end{cases}. \tag{66}$$

Using ω_i along with ς, a diagonal matrix $D(\omega_i,\varsigma)$ can be defined as

$$D(\omega_i,\varsigma) = \sqrt{p_i} S(-2\delta_i), \tag{67}$$

where

$$S(x) = diag\left(e^{\frac{-ix}{2}}, e^{\frac{ix}{2}}\right), \tag{68}$$

while p_i is evaluated via (65) as

$$p_i = |\delta_i|^2. \tag{69}$$

Finally, by exploiting Observation 3 of[145], leads to

$$U\left(\vec{\theta}\right) = WS(\delta_L)WS(\delta_{L-1})\dots WS(\delta_1), \tag{70}$$

where W is a matrix set as

$$W = \exp\left(i\pi\frac{X}{\mho}\right), \tag{71}$$

where $\mho$ is a coefficient, such that

$$WS\left(\delta_j\right) = U_j = U\left(X_j, \beta_j\right)U\left(Z_jZ_k, \gamma_j\right), \tag{72}$$

where δ_j is as given in (65) (with an index update).

Thus, the $\mathcal{D}(\mathcal{P}(A \to B))$ computational path is the map of the physical computational path

$$\mathcal{P}(A \to B) = U_L U_{L-1} \dots U_1 \tag{73}$$

formulated via the L nodes $V_1, \dots, V_L$ of N onto the correlation space, as

$$\mathcal{D}(\mathcal{P}(A \to B)) = WS(\delta_L)WS(\delta_{L-1})\dots WS(\delta_1). \tag{74}$$

Then using the system characterization of N of Section 2, reveals that $\mathcal{D}(N)$ is an extended correlation space with n computational paths, where an i-th computational path is evaluated as (74), thus the $\mathcal{D}(N)$ computational model of N is evaluated as

$$\begin{aligned}\mathcal{D}(N) =& \left(W_1S\left(\delta_{1,L}\right)W_1S\left(\delta_{1,L-1}\right)\dots W_1S\left(\delta_{1,1}\right)\right)\dots \\ &\dots\left(W_nS\left(\delta_{n,L}\right)W_nS\left(\delta_{n,L-1}\right)\dots W_nS\left(\delta_{n,1}\right)\right),\end{aligned} \tag{75}$$

where (i, j) identifies a j-th unitary of an i-th computational path $\mathcal{P}(A_i \to B_i)$, that concludes the proof. □

Objective function evaluation at multipartite entanglement. **Proposition 4** *Let $F_{\mathcal{P}(A\to B)}$ be the target function at a given objective function $C_{\mathcal{P}(A\to B)}$ evaluated for the computational path $\mathcal{P}(A \to B)$ via (58), as*

$$\begin{aligned}F_{\mathcal{P}(A\to B)} &= \sum_{\langle jk\rangle\in\mathcal{P}(A\to B)} F_{\langle jk\rangle} \\ &= \max_{\forall\theta}\left\langle\varphi^*\right| C_{\mathcal{P}(A\to B)}\left|\varphi^*\right\rangle \\ &= \left(-\tfrac{1}{2}\right)\max_{\forall\langle jk\rangle\in\mathcal{P}(A\to B)}\left(\sum_{\langle jk\rangle\in\mathcal{P}(A\to B)}\left\langle\varphi^*_{N,jk}\right| Z_jZ_k\left|\varphi^*_{N,jk}\right\rangle\right),\end{aligned} \tag{76}$$

where $C_{\mathcal{P}(A\to B)}$ is defined as

$$C_{\mathcal{P}(A\to B)} = \sum_{\langle jk\rangle\in\mathcal{P}(A\to B)} C_{jk}. \tag{77}$$

Theorem 2 (Scaling via gate parameters of unitaries). *The $F_{\mathcal{P}(A\to B)}$ target function of a computational path $\mathcal{P}(A \to B)$ with objective function $C_{\mathcal{P}(A\to B)} = \sum_{\langle jk\rangle\in\mathcal{P}(A\to B)} C_{jk}$ is maximized at gate parameters $\beta_j = \frac{\pi}{8}$ and $\gamma_{jk} = \frac{1}{2}\cos^{-1}\left(\frac{\Gamma_j-1}{\Gamma_j+1}\right)$ in the L nodes, where Γ_j is the number of remote entangled connections of j.*

Proof The proof utilizes the system model of Section 2, and focuses on a particular computational path $\mathcal{P}(A \to B)$ with an $C_{\mathcal{P}(A\to B)}$ objective function of a computational problem.

At $L-1$ entangled connections, $F_{\mathcal{P}(A\to B)}$ from (76) can be written as

$$F_{\mathcal{P}(A\to B)} = \tfrac{1}{2}\sum_{j=1}^{L-1}\zeta_{E_j}, \tag{78}$$

where ζ_{E_j} is the contribution of an l-level E_j entangled connection between qubits j and k in target function $F_{\mathcal{P}(A\to B)}$, defined as

$$\zeta_{E_j} = \left(\sin\left(2\beta_j + 2\beta_k\right)\right)\sin\gamma_{jk}\prod_{k=1}^{\Gamma_j+1}\cos\gamma_{jk}, \tag{79}$$

where Γ_j is the number of remote neighbor entangled qubits of j such that not neighbors of qubit k, while β_j, β_k and γ_{jk} are the gate parameters of unitaries of U_{xy} in (13) (The evaluation of (79) utilizes an abstraction. The structure of the distributed system is mapped onto a grid such that the vertices of the grid represent the qubits in the nodes, while an edge between the qubits identifies an l-level E_j entangled connection in the distributed system. Since all connections between the qubits are entangled, the vertices on the grid are separated only by the particular edge that directly connects the qubits, thus the distance between the qubits on the grid is set to unit for all connections[14].)

Assuming that γ_{jk} is set to the same value for all k, $k = 1,\ldots,\Gamma_j + 1$, at $\beta_j = \beta_k$ the result in (79) can be simplified as

$$\zeta_{E_j} = \left(\sin 4\beta_j\right)\sin\gamma_{jk}\cos^{(\Gamma_j+1)}\gamma_{jk}. \tag{80}$$

To verify (79), we first rewrite (56) for a particular entangled connection E_j, as

$$\begin{aligned} F_{\langle jk\rangle} &= \left(-\tfrac{1}{2}\right)\left\langle\varphi^*_{N,jk}\right| Z_jZ_k\left|\varphi^*_{N,jk}\right\rangle \\ &= \left(-\tfrac{1}{2}\right)\langle s|U^\dagger\left(N,\gamma_{jk}\right)\left(U^\dagger\left(\beta_j,X_j\right)Z_jU\left(\beta_j,X_j\right)\right)\left(U^\dagger(\beta_k,X_k)Z_kU(\beta_k,X_k)\right)U\left(N,\gamma_{jk}\right)|+\rangle, \end{aligned} \tag{81}$$

where $\left|\varphi^*_{N,jk}\right\rangle$ is the target state from (57), and

$$U\left(\beta_j,X_j\right) = \exp\left(-i\beta_jX_j\right) = \cos\left(\beta_j\right)I - i\sin\left(\beta_j\right)X_j \tag{82}$$

and

$$U\left(N,\gamma_{jk}\right) = \exp\left(-i\gamma_{jk}Z_jZ_k\right) = \cos\left(\gamma_{jk}\right)I - i\sin\left(\gamma_{jk}\right)Z_jZ_k, \tag{83}$$

where N is a product of pairs of Z operators[12,14].

Then,

$$\begin{aligned} &U^\dagger\left(\beta_j,X_j\right)Z_jU\left(\beta_j,X_j\right)\left(U^\dagger(\beta_k,X_k)Z_kU(\beta_k,X_k)\right) \\ &\quad= \exp\left(i\beta_jX_j\right)Z_j\exp\left(-i\beta_jX_j\right)\exp\left(i\beta_kX_k\right)Z_k\exp\left(-i\beta_kX_k\right), \end{aligned} \tag{84}$$

where

$$\begin{aligned} &\exp\left(i\beta_jX_j\right)Z_j\exp\left(-i\beta_jX_j\right) \\ &= \left(\cos\left(\beta_j\right)I + i\sin\left(\beta_j\right)X_j\right)Z_j\left(\cos\left(\beta_j\right)I - i\sin\left(\beta_j\right)X_j\right) \\ &= \left(\cos\left(\beta_j\right)Z_j + i\sin\left(\beta_j\right)Z_jX_j\right)\left(\cos\left(\beta_j\right)I - i\sin\left(\beta_j\right)X_j\right) \\ &= \left(\cos\left(\beta_j\right)Z_j + i\sin\left(\beta_j\right)Y_j\right)\left(\cos\left(\beta_j\right)I - i\sin\left(\beta_j\right)X_j\right) \\ &= \cos^2\left(\beta_j\right)Z_j - i\cos\left(\beta_j\right)\sin\left(\beta_j\right)Z_jX_j + i\cos\left(\beta_j\right)\sin\left(\beta_j\right)Y_j - i^2\sin^2\left(\beta_j\right)Y_jX_j \\ &= \cos^2\left(\beta_j\right)Z_j + i\cos\left(\beta_j\right)\sin\left(\beta_j\right)X_jZ_j + i\cos\left(\beta_j\right)\sin\left(\beta_j\right)Y_j - i^2\sin^2\left(\beta_j\right)Y_jX_j \\ &= \cos^2\left(\beta_j\right)Z_j + i\cos\left(\beta_j\right)\sin\left(\beta_j\right)Y_j + i\cos\left(\beta_j\right)\sin\left(\beta_j\right)Y_j + i^2\sin^2\left(\beta_j\right)Z_j \\ &= \left(\cos^2\left(\beta_j\right)Z_j + i^2\sin^2\left(\beta_j\right)Z_j\right) + 2i\cos\left(\beta_j\right)\sin\left(\beta_j\right)Y_j \\ &= \left(\tfrac{1}{2}\left(1+\cos\left(2\beta_j\right)\right)Z_j - \tfrac{1}{2}\left(1-\cos\left(2\beta_j\right)\right)Z_j\right) + 2i\left(\tfrac{1}{2}\left(\sin\left(2\beta_j\right)-\sin\left(0\right)\right)\right)Y_j \\ &= \left(\tfrac{1}{2}Z_j + \tfrac{1}{2}\cos\left(2\beta_j\right)Z_j - \tfrac{1}{2}Z_j + \tfrac{1}{2}\cos\left(2\beta_j\right)Z_j\right) + i\sin\left(2\beta_j\right)Y_j \\ &= Z_j\cos\left(2\beta_j\right) + iY_j\sin\left(2\beta_j\right), \end{aligned} \tag{85}$$

and

$$
\begin{aligned}
&\exp(i\beta_k X_k) Z_k \exp(-i\beta_k X_k) \\
&= (\cos(\beta_k) I + i \sin(\beta_k) X_k) Z_k (\cos(\beta_k) I - i \sin(\beta_k) X_k) \\
&= \left(\cos(\beta_k) Z_j + i \sin(\beta_k) Z_k X_k\right) (\cos(\beta_k) I - i \sin(\beta_k) X_k) \\
&= (\cos(\beta_k) Z_k + i \sin(\beta_k) Y_k)(\cos(\beta_k) I - i \sin(\beta_k) X_k) \\
&= \cos^2(\beta_k) Z_k - i \cos(\beta_k) \sin(\beta_k) Z_j X_j + i \cos(\beta_k) \sin(\beta_k) Y_k - i^2 \sin^2(\beta_k) Y_k X_k \\
&= \cos^2(\beta_k) Z_k + i \cos(\beta_k) \sin(\beta_k) X_j Z_j + i \cos(\beta_k) \sin(\beta_k) Y_k - i^2 \sin^2(\beta_k) Y_k X_k \\
&= \cos^2(\beta_k) Z_k + i \cos(\beta_k) \sin(\beta_k) Y_k + i \cos(\beta_k) \sin(\beta_k) Y_k + i^2 \sin^2(\beta_k) Z_k \\
&= \left(\cos^2(\beta_k) Z_k + i^2 \sin^2(\beta_k) Z_k\right) + 2i \cos(\beta_k) \sin(\beta) Y_k \\
&= \left(\tfrac{1}{2}(1 + \cos(2\beta_k)) Z_k - \tfrac{1}{2}(1 - \cos(2\beta_k)) Z_k\right) + 2i\left(\tfrac{1}{2}(\sin(2\beta_k) - \sin(0))\right) Y_k \\
&= \left(\tfrac{1}{2} Z_k + \tfrac{1}{2} \cos(2\beta_k) Z_k - \tfrac{1}{2} Z_k + \tfrac{1}{2} \cos(2\beta_k) Z_k\right) + i \sin(2\beta_k) Y_k \\
&= Z_k \cos(2\beta_k) + i Y_k \sin(2\beta_k),
\end{aligned}
\tag{86}
$$

thus

$$
\begin{aligned}
&U^\dagger(\beta_j, X_j) Z_j U(\beta_j, X_j) U^\dagger(\beta_k, X_k) Z_k U(\beta_k, X_k) \\
&\quad = \left(Z_j \cos(2\beta_j) + i Y_j \sin(2\beta_j)\right)(Z_k \cos(2\beta_k) + i Y_k \sin(2\beta_k)).
\end{aligned}
\tag{87}
$$

Assuming, that $\beta_j = \beta_k = \beta$, (87) can be written in a simplified form as

$$
\begin{aligned}
&U(\beta, X)^\dagger Z_j Z_k U(\beta, X) \\
&= U^\dagger(\beta_j, X_j) Z_j U(\beta_j, X_j) U^\dagger(\beta_k, X_k) Z_k U(\beta_k, X_k) \\
&= \cos^2(2\beta) Z_j Z_k + i \cos(2\beta) \sin(2\beta) Z_j Y_k + i \cos(2\beta) \sin(2\beta) Y_j Z_k + i^2 \sin^2(2\beta) Y_j Y_k.
\end{aligned}
\tag{88}
$$

The related terms $U(N, \gamma_{jk}) Z_j U^\dagger(N, \gamma_{jk})$ and $U(N, \gamma_{jk}) Y_j U^\dagger(N, \gamma_{jk})$ of (81) are evaluated as

$$
\begin{aligned}
&U(N, \gamma_{jk}) Z_j U^\dagger(N, \gamma_{jk}) \\
&= \left(\cos(\gamma_{jk}) I - i \sin(\gamma_{jk}) Z_j Z_k\right) Z_j \left(\cos(\gamma_{jk}) I + i \sin(\gamma_{jk}) Z_j Z_k\right) \\
&= \left(Z_j \cos(\gamma_{jk}) I - i Z_j \sin(\gamma_{jk}) Z_j Z_k\right)\left(\cos(\gamma_{jk}) I + i \sin(\gamma_{jk}) Z_j Z_k\right) \\
&= \left(\cos(\gamma_{jk}) Z_j - i \sin(\gamma_{jk}) Z_k\right)\left(\cos(\gamma_{jk}) I + i \sin(\gamma_{jk}) Z_j Z_k\right) \\
&= \cos^2(\gamma_{jk}) Z_j + i \cos(\gamma_{jk}) \sin(\gamma_{jk}) Z_k - i \cos(\gamma_{jk}) \sin(\gamma_{jk}) Z_k - i^2 \sin^2(\gamma_{jk}) Z_j \\
&= \cos^2(\gamma_{jk}) Z_j - i^2 \sin^2(\gamma_{jk}) Z_j \\
&= \cos^2(\gamma_{jk}) Z_j + \sin^2(\gamma_{jk}) Z_j \\
&= \tfrac{1}{2}\left(1 + \cos(2\gamma_{jk})\right) Z_j + \tfrac{1}{2}\left(1 - \cos(2\gamma_{jk})\right) Z_j \\
&= \tfrac{1}{2} Z_j + \cos(2\gamma_{jk}) Z_j + \tfrac{1}{2} Z_j - \cos(2\gamma_{jk}) Z_j \\
&= Z_j,
\end{aligned}
\tag{89}
$$

and

$$
\begin{aligned}
&U(N, \gamma_{jk}) Y_j U^\dagger(N, \gamma_{jk}) \\
&= \left(\cos(\gamma_{jk}) I - i \sin(\gamma_{jk}) Z_j Z_k\right) Y_j \left(\cos(\gamma_{jk}) I + i \sin(\gamma_{jk}) Z_j Z_k\right) \\
&= \left(\cos(\gamma_{jk}) Y_j - i \sin(\gamma_{jk}) Y_j Z_j Z_k\right)\left(\cos(\gamma_{jk}) I + i \sin(\gamma_{jk}) Z_j Z_k\right) \\
&= \left(\cos(\gamma_{jk}) Y_j - i \sin(\gamma_{jk}) X_j Z_k\right)\left(\cos(\gamma_{jk}) I + i \sin(\gamma_{jk}) Z_j Z_k\right) \\
&= \cos^2(\gamma_{jk}) Y_j + i \cos(\gamma_{jk}) \sin(\gamma_{jk}) Y_j Z_j Z_k - i \sin(\gamma_{jk}) \cos(\gamma_{jk}) X_j Z_k - i^2 \sin^2(\gamma_{jk}) (X_j Z_k Z_j Z_k) \\
&= \cos^2(\gamma_{jk}) Y_j - i \cos(\gamma_{jk}) \sin(\gamma_{jk}) (X_j Z_j) Z_j Z_k - i \sin(\gamma_{jk}) \cos(\gamma_{jk}) X_j Z_k + i^2 \sin^2(\gamma_{jk}) (Y_j) \\
&= \cos^2(\gamma_{jk}) Y_j - i \cos(\gamma_{jk}) \sin(\gamma_{jk}) X_j Z_k - i \sin(\gamma_{jk}) \cos(\gamma_{jk}) X_j Z_k + i^2 \sin^2(\gamma_{jk}) (Y_j) \\
&= \left(\tfrac{1}{2}\left(1 + \cos(2\gamma_{jk})\right) Y_j - \tfrac{1}{2}\left(1 - \cos(2\gamma_{jk})\right) Y_j\right) - 2i\left(\tfrac{1}{2}\left(\sin(2\gamma_{jk}) - \sin(0)\right)\right) X_j Z_k \\
&= \left(\tfrac{1}{2} Y_j + \tfrac{1}{2} \cos(2\gamma_{jk}) Y_j - \tfrac{1}{2} Y_j + \tfrac{1}{2} \cos(2\gamma_{jk}) Y_j\right) - 2i\left(\tfrac{1}{2}\left(\sin(2\gamma_{jk}) - \sin(0)\right)\right) X_j Z_k \\
&= Y_j \cos(2\gamma_{jk}) - i X_j Z_k \sin(2\gamma_{jk}).
\end{aligned}
\tag{90}
$$

Then, using (81), let χ_{jk} be defined as

$$\chi_{jk} = U^{\dagger}(N, \gamma_{jk})\left(U^{\dagger}(\beta_j, X_j) Z_j U(\beta_j, X_j)\right)\left(U^{\dagger}(\beta_k, X_k) Z_k U(\beta_k, X_k)\right) U(N, \gamma_{jk}) \tag{91}$$

thus (81) can be rewritten as

$$F_{\langle jk \rangle} = \left(-\tfrac{1}{2}\right)\langle + | \chi_{jk} | + \rangle, \tag{92}$$

with

$$\langle + | X | + \rangle = 1, \tag{93}$$

and

$$\langle + | Z | + \rangle = \langle + | Y | + \rangle = 0. \tag{94}$$

It can be verified[14], that χ_{jk} can be decomposed as

$$\chi_{jk} = \eta_j \eta_k, \tag{95}$$

where

$$\begin{aligned} \eta_j &= Z_j \cos 2\beta_j + \left(Y_j \cos \gamma_{jk} - X_j Z_k \sin \gamma_{jk}\right) \sin 2\beta_j \prod_{k=1}^{\Gamma_j + 1} \cos \gamma_{jk} \\ &= Z_j \cos 2\beta_j + \left(Y_j \sin 2\beta_j \prod_{k=1}^{\Gamma_j} \cos \gamma_{jk} - X_j Z_k \sin \gamma_{jk} \sin 2\beta_j \prod_{k=1}^{\Gamma_j + 1} \cos \gamma_{jk} \right) \end{aligned} \tag{96}$$

and

$$\begin{aligned} \eta_k &= Z_k \cos 2\beta_k + \left(Y_k \cos \gamma_{jk} - X_k Z_j \sin \gamma_{jk}\right) \sin 2\beta_k \prod_{k=1}^{\Gamma_j + 1} \cos \gamma_{jk} \\ &= Z_k \cos 2\beta_k + \left(Y_k \sin 2\beta_k \prod_{k=1}^{\Gamma_j} \cos \gamma_{jk} - X_k Z_j \sin \gamma_{jk} \sin 2\beta_k \prod_{k=1}^{\Gamma_j + 1} \cos \gamma_{jk} \right). \end{aligned} \tag{97}$$

Thus, χ_{jk} can be evaluated as

$$
\begin{aligned}
\chi_{jk} =& \left(Z_j \cos 2\beta_j + Y_j \sin 2\beta_j \prod_{k=1}^{\Gamma_j} \cos\gamma_{jk} - X_j Z_k \sin\gamma_{jk} \sin 2\beta_j \prod_{k=1}^{\Gamma_j+1} \cos\gamma_{jk} \right) \\
& \times \left(Z_k \cos 2\beta_k + Y_k \sin 2\beta_k \prod_{k=1}^{\Gamma_j} \cos\gamma_{jk} - X_k Z_j \sin\gamma_{jk} \sin 2\beta_k \prod_{k=1}^{\Gamma_j+1} \cos\gamma_{jk} \right) \\
=& Z_j Z_k \cos 2\beta_j \cos 2\beta_k + Z_j Y_k \cos 2\beta_j \sin 2\beta_k \prod_{k=1}^{\Gamma_j} \cos\gamma_{jk} \\
& - X_k \cos 2\beta_j \sin\gamma_{jk} \sin 2\beta_k \prod_{k=1}^{\Gamma_j+1} \cos\gamma_{jk} \\
& + Y_j Z_k \sin 2\beta_j \prod_{k=1}^{\Gamma_j} \cos\gamma_{jk} \cos 2\beta_k + Y_j Y_k \sin 2\beta_j \sin 2\beta_k \prod_{k=1}^{2\Gamma_j} \cos\gamma_{jk} \\
& - Y_j Z_j X_k \sin\gamma_{jk} \sin 2\beta_j \sin 2\beta_k \prod_{k=1}^{2\Gamma_j+1} \cos\gamma_{jk} \\
& - X_j \sin\gamma_{jk} \sin 2\beta_j \cos 2\beta_k \prod_{k=1}^{\Gamma_j+1} \cos\gamma_{jk} - X_j Z_k Y_k \sin\gamma_{jk} \sin 2\beta_j \sin 2\beta_k \prod_{k=1}^{2\Gamma_j+1} \cos\gamma_{jk} \\
& + X_j Z_j Z_k X_k \sin^2\gamma_{jk} \sin 2\beta_j \sin 2\beta_k \prod_{k=1}^{2(\Gamma_j+1)} \cos\gamma_{jk} \\
=& Z_j Z_k \cos 2\beta_j \cos 2\beta_k + Z_j Y_k \cos 2\beta_j \sin 2\beta_k \prod_{k=1}^{\Gamma_j} \cos\gamma_{jk} \\
& - X_k \cos 2\beta_j \sin\gamma_{jk} \sin 2\beta_k \prod_{k=1}^{\Gamma_j+1} \cos\gamma_{jk} + Y_j Z_k \sin 2\beta_j \prod_{k=1}^{\Gamma_j} \cos\gamma_{jk} \cos 2\beta_k \\
& + Y_j Y_k \sin 2\beta_j \sin 2\beta_k \prod_{k=1}^{2\Gamma_j} \cos\gamma_{jk} - X_j X_k \sin\gamma_{jk} \sin 2\beta_j \sin 2\beta_k \prod_{k=1}^{2\Gamma_j+1} \cos\gamma_{jk} \\
& - X_j \sin\gamma_{jk} \sin 2\beta_j \cos 2\beta_k \prod_{k=1}^{\Gamma_j+1} \cos\gamma_{jk} + X_j X_k \sin\gamma_{jk} \sin 2\beta_j \sin 2\beta_k \prod_{k=1}^{2\Gamma_j+1} \cos\gamma_{jk} \\
& - Y_j Y_k \sin^2\gamma_{jk} \sin 2\beta_j \sin 2\beta_k \prod_{k=1}^{2(\Gamma_j+1)} \cos\gamma_{jk}.
\end{aligned} \tag{98}
$$

Then, by utilizing the fact that input system $|+\rangle$, and therefore also $|s\rangle$, is an eigenstate of each X with eigenvalue 1[14] (see also (93) and (94)), the terms containing Y and Z vanish from (98), while X can be replaced as $X = 1$. As follows, (98) can be rewritten as

$$
\begin{aligned}
\chi_{jk} =& - X_k \cos 2\beta_j \sin\gamma_{jk} \sin 2\beta_k \prod_{k=1}^{\Gamma_j+1} \cos\gamma_{jk} \\
& - X_j X_k \sin\gamma_{jk} \sin 2\beta_j \sin 2\beta_k \prod_{k=1}^{2\Gamma_j+1} \cos\gamma_{jk} \\
& - X_j \cos 2\beta_k \sin\gamma_{jk} \sin 2\beta_j \prod_{k=1}^{\Gamma_j+1} \cos\gamma_{jk} + X_j X_k \sin\gamma_{jk} \sin 2\beta_j \sin 2\beta_k \prod_{k=1}^{2\Gamma_j+1} \cos\gamma_{jk} \\
=& - \left(X_k \cos 2\beta_j \sin\gamma_{jk} \sin 2\beta_k \prod_{k=1}^{\Gamma_j+1} \cos\gamma_{jk} + X_j \cos 2\beta_k \sin\gamma_{jk} \sin 2\beta_j \prod_{k=1}^{\Gamma_j+1} \cos\gamma_{jk} \right) \\
=& - \left(\cos 2\beta_j \sin\gamma_{jk} \sin 2\beta_k \prod_{k=1}^{\Gamma_j+1} \cos\gamma_{jk} + \cos 2\beta_k \sin\gamma_{jk} \sin 2\beta_j \prod_{k=1}^{\Gamma_j+1} \cos\gamma_{jk} \right).
\end{aligned} \tag{99}
$$

Further assuming that $\beta_j = \beta_k = \beta$ holds, (99) can be simplified as

$$\chi_{jk} = -2\cos 2\beta \sin\gamma_{jk} \sin 2\beta \prod_{k=1}^{\Gamma_j+1} \cos\gamma_{jk}. \tag{100}$$

Therefore, (92) is as

$$\begin{aligned} F_{\langle jk\rangle} &= -\tfrac{1}{2}\chi_{jk} \\ &= \tfrac{1}{2}\left(\cos 2\beta_j \sin 2\beta_k + \cos 2\beta_k \sin 2\beta_j\right)\left(\sin\gamma_{jk}\prod_{k=1}^{\Gamma_j+1}\cos\gamma_{jk}\right) \\ &= \tfrac{1}{2}\left(\sin\left(2\beta_j+2\beta_k\right) - \tfrac{1}{2}\sin\left(2\beta_j-2\beta_k\right) - \tfrac{1}{2}\sin\left(2\beta_k-2\beta_j\right)\right)\left(\sin\gamma_{jk}\prod_{k=1}^{\Gamma_j+1}\cos\gamma_{jk}\right) \\ &= \tfrac{1}{2}\sin\left(2\beta_j+2\beta_k\right)\left(\sin\gamma_{jk}\prod_{k=1}^{\Gamma_j+1}\cos\gamma_{jk}\right), \end{aligned} \tag{101}$$

which at condition $\beta_j = \beta_k = \beta$ (which is the case for a maximization) simplifies as

$$\begin{aligned} F_{\langle jk\rangle} &= \tfrac{1}{2}\sin(4\beta)\left(\sin\gamma_{jk}\prod_{k=1}^{\Gamma_j+1}\cos\gamma_{jk}\right) \\ &= \tfrac{1}{2}\zeta_{E_j}. \end{aligned} \tag{102}$$

Then, using (79), the $C_{\mathcal{P}(A\to B)}$ objective function of the $\mathcal{P}(A\to B)$ computational path is evaluated as

$$C_{\mathcal{P}(A\to B)} = \tfrac{1}{2}\phi_{\mathcal{P}(A\to B)} + \tfrac{1}{2}\sum_{j=1}^{L-1}\zeta_{E_j}, \tag{103}$$

where $\phi_{\mathcal{P}(A\to B)}$ identifies the total number of entangled connections of $\mathcal{P}(A\to B)$, as

$$\phi_{\mathcal{P}(A\to B)} = \tfrac{1}{2}\left(\sum_{j=1}^{L-1}\left(\Gamma_j+2\right)\right) + \tfrac{1}{2}, \tag{104}$$

where the term $+\frac{1}{2} = \frac{1}{2}(+1)$ indicates the coupling unitary $U_B^C = \exp\left(-itH^{(k,B)}\right)$ in node B in the evaluation $C_{\mathcal{P}(A\to B)}$, by a convention.

Assuming that (80) holds, (103) is simplified as

$$\begin{aligned} C_{\mathcal{P}(A\to B)} &= \tfrac{1}{4} + \tfrac{1}{4}\sum_{j=1}^{L-1}\left(\Gamma_j+2\right) + \tfrac{1}{2}\sum_{j=1}^{L-1}\left(\sin 4\beta_j\right)\sin\gamma_{jk}\cos^{(\Gamma_j+1)}\gamma_{jk} \\ &= \tfrac{1}{4} + \tfrac{1}{2}\sum_{j=1}^{L-1}\tfrac{1}{2}\left(\Gamma_j+2\right) + \left(\sin 4\beta_j\right)\sin\gamma_{jk}\cos^{(\Gamma_j+1)}\gamma_{jk}. \end{aligned} \tag{105}$$

If for each node the same β_j, γ_{jk} and Γ_j values are set, (105) can be rewritten as

$$C_{\mathcal{P}(A\to B)} = \tfrac{1}{4} + \tfrac{1}{2}(L-1)\left(\tfrac{1}{2}\left(\Gamma_j+2\right) + \left(\sin 4\beta_j\right)\sin\gamma_{jk}\cos^{(\Gamma_j+1)}\gamma_{jk}\right). \tag{106}$$

After some calculations, the gate-parameter values β_j and γ_{jk} that maximize ζ_{E_j} (and therefore $C_{\mathcal{P}(A\to B)}$) are at

$$4\cos 4\beta_j = 0 \tag{107}$$

and

$$\cos^{(\Gamma_j+2)}\gamma_{jk} - \left(\Gamma_j+1\right)\cos^{(\Gamma_j)}\gamma_{jk}\sin^2\gamma_{jk} = 0, \tag{108}$$

that yields gate parameter values

$$\beta_j = \tfrac{\pi}{8}, \tag{109}$$

and

$$\gamma_{jk} = \tfrac{1}{2}\cos^{-1}\left(\tfrac{\Gamma_j-1}{\Gamma_j+1}\right). \tag{110}$$

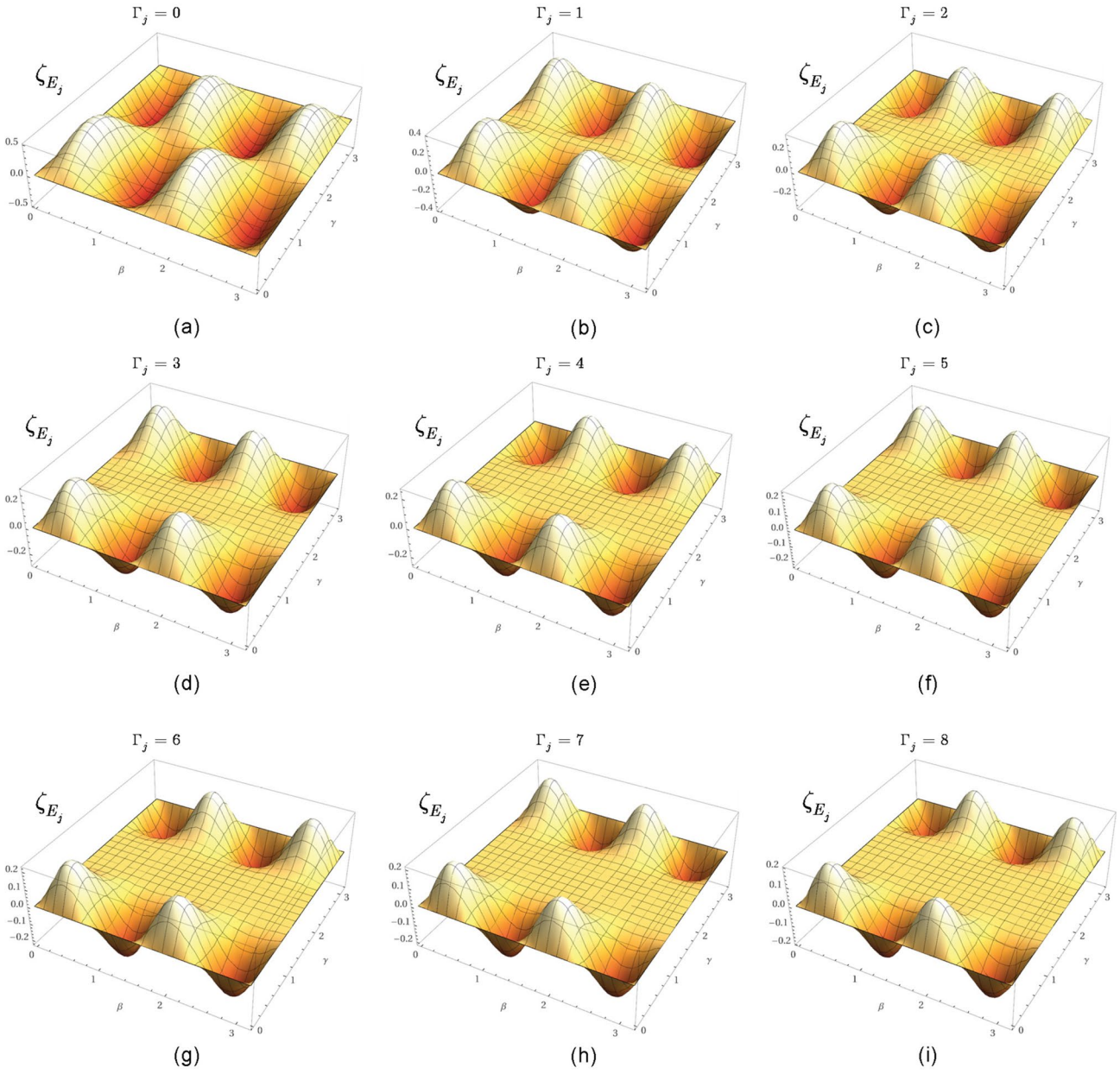

Figure 3. The values of ζ_{E_j} in function of gate parameters β_j and $\gamma_j = \frac{1}{2}\gamma_{jk}$, for different Γ_j values (γ_{jk} is set for the same value for all k, $k = 1, \ldots, \Gamma_j + 1$). (**a**) $\Gamma_j = 0$ (**b**) $\Gamma_j = 1$ (**c**) $\Gamma_j = 2$ (**d**) $\Gamma_j = 3$ (**e**) $\Gamma_j = 4$ (**f**) $\Gamma_j = 5$ (**g**) $\Gamma_j = 6$ (**h**) $\Gamma_j = 7$ (**i**) $\Gamma_j = 8$.

Thus, (102) is maximized as

$$F_{\langle jk \rangle} = \tfrac{1}{2}\sin\left(\tfrac{\pi}{2}\right)\left(\sin\left(\tfrac{1}{2}\cos^{-1}\left(\tfrac{\Gamma_j-1}{\Gamma_j+1}\right)\right)\prod_{k=1}^{\Gamma_j+1}\cos\left(\tfrac{1}{2}\cos^{-1}\left(\tfrac{\Gamma_j-1}{\Gamma_j+1}\right)\right)\right). \tag{111}$$

The maximized $C_{\mathcal{P}(A\to B)}$ objective function value of (105) for a given computational path is therefore

$$\begin{aligned} C_{\mathcal{P}(A\to B)} &= \tfrac{1}{4} + \tfrac{1}{2}\sum_{j=1}^{L-1}\tfrac{1}{2}(\Gamma_j+2) + \left(\sin\tfrac{\pi}{2}\right)\left(\sin\left(\tfrac{1}{2}\cos^{-1}\left(\tfrac{\Gamma_j-1}{\Gamma_j+1}\right)\right)\right)\cos^{(\Gamma_j+1)}\left(\tfrac{1}{2}\cos^{-1}\left(\tfrac{\Gamma_j-1}{\Gamma_j+1}\right)\right) \\ &= \tfrac{1}{4} + \tfrac{1}{2}\sum_{j=1}^{L-1}\tfrac{1}{2}(\Gamma_j+2) + \sin\left(\tfrac{\pi}{4} - \tfrac{1}{2}\sin^{-1}\left(\tfrac{\Gamma_j-1}{\Gamma_j+1}\right)\right)\cos^{(\Gamma_j+1)}\left(\tfrac{\pi}{4} - \tfrac{1}{2}\sin^{-1}\left(\tfrac{\Gamma_j-1}{\Gamma_j+1}\right)\right), \end{aligned} \tag{112}$$

and the maximized value of (106) is as

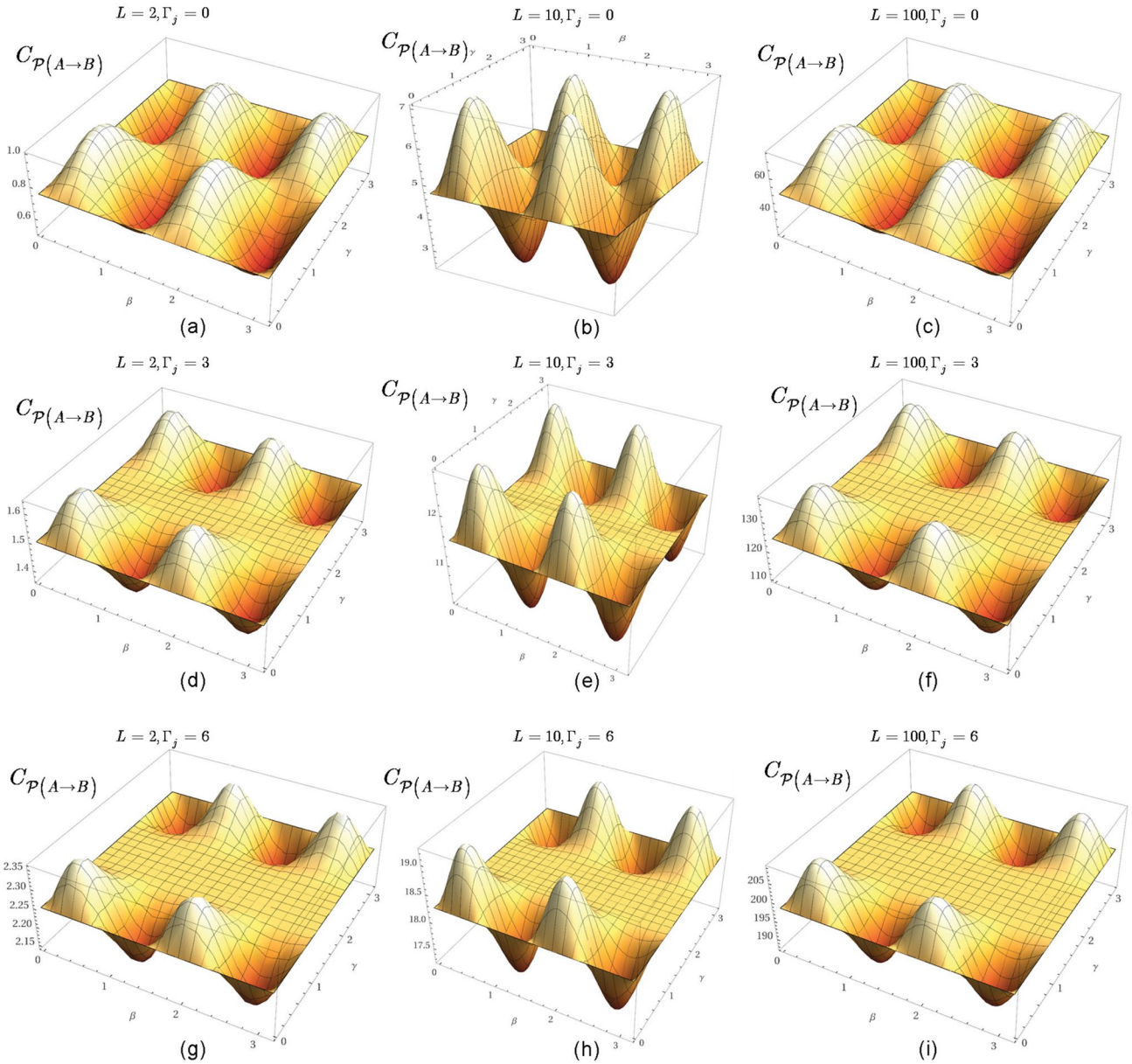

Figure 4. The $C_{\mathcal{P}(A\to B)}$ objective function values for a computational path $\mathcal{P}(A \to B)$ in function of gate parameters β_j and $\gamma_j = \frac{1}{2}\gamma_{jk}$, for different L and Γ_j (β_j and γ_j are set for the same values for all j, $j = 1, \ldots, L-1$ and k, $k = 1, \ldots, \Gamma_j + 1$). (**a**) $L = 2, \Gamma_j = 0$ (**b**) $L = 10, \Gamma_j = 0$ (**c**) $L = 100, \Gamma_j = 0$ (**d**) $L = 2, \Gamma_j = 3$ (**e**) $L = 10, \Gamma_j = 3$ (**f**) $L = 100, \Gamma_j = 3$ (**g**) $L = 2, \Gamma_j = 6$ (**h**) $L = 10, \Gamma_j = 6$ (**i**) $L = 100, \Gamma_j = 6$.

$$C_{\mathcal{P}(A\to B)} = \tfrac{1}{4} + \tfrac{1}{2}(L-1)\left(\tfrac{1}{2}(\Gamma_j+2) + \sin\left(\tfrac{\pi}{4} - \tfrac{1}{2}\sin^{-1}\left(\tfrac{\Gamma_j-1}{\Gamma_j+1}\right)\right)\cos^{(\Gamma_j+1)}\left(\tfrac{\pi}{4} - \tfrac{1}{2}\sin^{-1}\left(\tfrac{\Gamma_j-1}{\Gamma_j+1}\right)\right)\right). \tag{113}$$

The proof is concluded here. □

The values of ζ_{E_j} in function of gate parameters β_j and $\gamma_j = \frac{1}{2}\gamma_{jk}$, for different Γ_j values (γ_{jk} is set for the same value for all k, $k = 1, \ldots, \Gamma_j + 1$) are depicted in Fig. 3.

The objective function values (106) for a computational path $\mathcal{P}(A \to B)$ in function of gate parameters β_j and $\gamma_j = \frac{1}{2}\gamma_{jk}$, at different L node number and Γ_j values (β_j and γ_j are set as the same for all j, $j = 1, \ldots, L-1$ and k, $k = 1, \ldots, \Gamma_j + 1$) are depicted in Fig. 4.

The gate parameter values β_j and γ_{jk} for the maximization of ζ_{E_j} are depicted in Fig. 5.

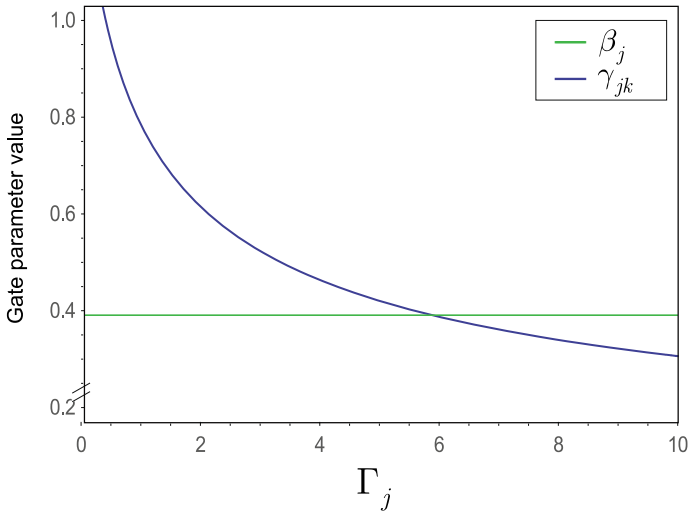

Figure 5. Gate parameter values β_j and γ_{jk} in function of Γ_j for the maximization of ζ_{E_j} in the distributed system N.

Scaling of a distributed quantum processing

Target function scaling at a decoherence. Let $\mathcal{S}_{\varphi^*_{N,jk}}(t)$ be the time evolution[146] of target state $\left|\varphi^*_{N,jk}(t)\right\rangle$ defined at a particular t, as

$$\begin{aligned}\mathcal{S}_{\varphi^*_{N,jk}}(t) &= \left|\left\langle \varphi^*_{N,jk}(t_0)\middle|\varphi^*_{N,jk}(t)\right\rangle\right|^2 \\ &= |\mathcal{A}(t)|^2,\end{aligned} \tag{114}$$

where $\left|\varphi^*_{N,jk}(t)\right\rangle$ is defined via (57), as a target state at t, as

$$\begin{aligned}\left|\varphi^*_{N,jk}(t)\right\rangle &= \left|\gamma_{jk}(t),\beta_k(t),\beta_j(t),N\right\rangle \\ &= U\big(B,\beta_j(t)\big)U(B,\beta_k(t))U\big(N,\gamma_{jk}(t)\big)|s\rangle,\end{aligned} \tag{115}$$

where $\beta_j(t)$, $\beta_k(t)$ and $\gamma_{jk}(t)$ are values of the gate parameters at a given time t associated to $\langle ij\rangle$, while $\left|\varphi^*_{N,jk}(t_0)\right\rangle$ is an initial state at some $t_0 \in [0,T]$, while $\mathcal{A}(t)$ is the survival amplitude[146,147], defined as

$$\mathcal{A}(t) = \left\langle \varphi^*_{N,jk}(t_0)\middle|\,\hat{U}(t,t_0)\middle|\varphi^*_{N,jk}(t_0)\right\rangle, \tag{116}$$

where $\hat{U}(t,t_0)$ is the time evolution operator generated by a Hamiltonian $\hat{H}$, as

$$\hat{U}(t,t_0) = T\exp\left(-i\int_{t_0}^{t} dx\hat{H}(x)\Big/\hbar\right). \tag{117}$$

From the exponential decay law[147], (116) can be written as

$$\mathcal{A}(t) = e^{-\Delta t}, \tag{118}$$

where Δ is the decay rate[146].

Proposition 5 *The $F_{\langle jk\rangle}(t)$ is the target function $F_{\langle jk\rangle}$ from (56) at a given t, defined as*

$$F_{\langle jk\rangle}(t) = \max_{\forall\theta}\left(\left(-\tfrac{1}{2}\right)\left\langle\varphi^*_{N,jk}(t)\middle|Z_jZ_k\middle|\varphi^*_{N,jk}(t)\right\rangle\right). \tag{119}$$

Theorem 3 (Target function scaling at decoherence). *At an systemal decoherence, for any non-zero quantum decay Δ on $\langle ij\rangle$, the $F(\langle ij\rangle)$ target function is scalable via the local $M[m_b]$ measurement operator of the $\mathcal{L}_D$ download procedure.*

Proof Let assume that the total number of entangled connections of N is $D = n(L-1)$. Then, let $t_{\langle ij\rangle}(N)$ be a vector of initialization time parameters of the target states of the entangled connections, defined as

$$t_{\langle ij\rangle}(N) = \left(t_0^{(1)}, \ldots, t_0^{(D)}\right)^T, \tag{120}$$

where $t_0^{(j)} \in [0, T]$ is the initialization time (an initial time value when the target state is prepared) of target state $\left|\varphi^*_{N,jk}(t_0)\right\rangle$, $j = 1, \ldots, D$.

For the survival amplitudes of the system states associated to the entangled connections at a given t, we also define a $\mathcal{A}_N(t)$ vector of survival amplitudes associated to the D target states, as

$$\mathcal{A}_N(t) = \left(\mathcal{A}^{(1)}(t), \ldots, \mathcal{A}^{(D)}(t)\right)^T = \left(e^{-\Delta_1 t}, \ldots, e^{-\Delta_D t}\right)^T, \tag{121}$$

where $\mathcal{A}^{(j)}(t)$ is the survival amplitude of $\left|\varphi^*_{N,jk}(t)\right\rangle$, while Δ_j is the decay rate belongs to $\mathcal{A}^{(j)}(t)$ defined via $\hat{U}\left(t, t_0^{(j)}\right)$ that evolves $\left|\varphi^*_{N,jk}\left(t_0^{(j)}\right)\right\rangle$ to $\left|\varphi^*_{N,jk}(t)\right\rangle$.

Then, let $\mathcal{L}_D$ be a downloading procedure that requires the utilization of $M[m_b]$ local measurements for the localization onto the target nodes with a measurement vector $M(N)$, as

$$M(N) = \left(M\left(\tau^{(1)}\right)[m_b], \ldots, M\left(\tau^{(2D)}\right)[m_b]\right)^T, \tag{122}$$

where $M\left(\tau^{(j)}\right)[m_b]$ identifies a measurement $M[m_b]$ on qubit j of $\langle jk\rangle$ at time $\tau^{(i)} \in [0, T]$ in $N, i = 1, \ldots, 2D$, as

$$M\left(\tau^{(j)}\right)[m_b] = \begin{cases} 1, \text{if } j \text{ is measured at } \tau^{(j)} \\ 0, \text{otherwise.} \end{cases} \tag{123}$$

Using (118), for a given qubit j, we define the $\mu_j(t)$ cumulated target state intensity which is dynamic term to model the interaction within the entangled network structure, as follows. Term $\mu_j(t)$ is defined as the sum of weighted target state decoherence terms (weighted target state intensities) of existing neighboring entangled connections and the actual weighted target state intensity at a local decoherence (local target function intensity), as

$$\begin{aligned} \mu_j(t) &= \Lambda_{\langle jk\rangle}\left(t, t_0^{(j)}\right) + \sum_{l=1, l\neq k}^{\Gamma_j+1} \Lambda_{\langle jl\rangle}\left(t, t_0^{(l)} < t\right) \\ &= F_{\langle jk\rangle}\left(t_0^{(j)}\right)\mathcal{A}_j\left(t, t_0^{(j)}\right) + \sum_{l=1, l\neq k}^{\Gamma_j+1} \int_0^t \Lambda_{\langle jl\rangle}(t, s) dG_l(s) \\ &= F_{\langle jk\rangle}\left(t_0^{(j)}\right)\mathcal{A}_j\left(t, t_0^{(j)}\right) + \sum_{l=1, l\neq k}^{\Gamma_j+1} \int_0^t F_{\langle jl\rangle}\left(t_0^{(l)}\right)\mathcal{A}_l(t, s) dG_l(s) \\ &= F_{\langle jk\rangle}\left(t_0^{(j)}\right)e^{-\Delta_j\left(t-t_0^{(j)}\right)} + \sum_{l=1, l\neq k}^{\Gamma_j+1} \int_0^t F_{\langle jl\rangle}\left(t_0^{(l)}\right)e^{-\Delta_l(t-s)} dG_l(s), \end{aligned} \tag{124}$$

where term $\Lambda_{\langle jk\rangle}\left(t, t_0^{(j)}\right)$ is defined as the intensity of a target state $\left|\varphi^*_{N,jk}(t)\right\rangle$,

$$\begin{aligned} \Lambda_{\langle jk\rangle}\left(t, t_0^{(j)}\right) &= F_{\langle jk\rangle}\left(t_0^{(j)}\right)\mathcal{A}_j\left(t, t_0^{(j)}\right) \\ &= F_{\langle jk\rangle}\left(t_0^{(j)}\right)e^{-\Delta_j\left(t-t_0^{(j)}\right)}, \end{aligned} \tag{125}$$

where $\mathcal{A}_j\left(t, t_0^{(j)}\right) = e^{-\Delta_j\left(t-t_0^{(j)}\right)}$ is the survival amplitude of $\left|\varphi^*_{N,jk}(t)\right\rangle$ such that the target state is initialized at $t_0^{(j)}$, $F_{\langle jk\rangle}\left(t_0^{(j)}\right)$ is the initial target function value at $t_0^{(j)}$, while $\langle jl\rangle$ refer to the neighboring entangled connections of $j, l = 1, \ldots, \left(\Gamma_j + 2\right) - 1, l \neq k$, while $G_l(s)$ is a control parameter[148], defined as

$$G_l(s) = \begin{cases} 0, \text{if } s < t_0^{(l)} \\ 1, \text{if } s \geq t_0^{(l)} \end{cases}, \tag{126}$$

where $s \leq T$.

Using (124), the $\mu_N(t) = (\mu_1(t), \ldots, \mu_D(t))^T$ cumulated target state intensity of N can be defined as

$$\mu_N(t) = \Lambda_N(t) + \int_0^t F_N(t_0)\mathcal{A}_N(t, s) dG_N(s), \tag{127}$$

where $\Lambda_N(t)$ is the vector of target state intensities of N

$$\Lambda_N(t) = \Lambda_1\left(t, t_0^{(1)}\right), \ldots, \Lambda_D\left(t, t_0^{(D)}\right)^T, \tag{128}$$

and

$$\begin{aligned} F_N(t_0)\mathcal{A}_N(t,s) &= \left[F_{\langle jl\rangle}\left(t_0^{(l)}\right)\mathcal{A}_l(t,s)\right]_{j,l=1,\ldots,l=\Gamma_j+1,l\neq k} \\ &= \left[F_{\langle jl\rangle}\left(t_0^{(l)}\right)e^{-\Delta_l(t-s)}\right]_{j,l=1,\ldots,l=\Gamma_j+1,l\neq k}, \end{aligned} \tag{129}$$

while $G_N(s)$ is a vector of control parameters

$$G_N(s) = (G_1(t), \ldots, G_D(t))^T. \tag{130}$$

At that point, our aim is to reveal the impacts of a $M[m_b]$ local measurement (performed in the $\mathcal{L}_D$ download phase) on the $\mu_N(t)$ cumulated target function intensity (127), i.e., to describe the impact of a local measurement and the localization process on the global entangled network structure.

Let us assume that a $M[m_b]$ measurement is performed on a qubit j of $\langle jk\rangle$ at $\tau^{(j)} \in [0, T]$, denoted by $M\left(\tau^{(j)}\right)[m_b]$. Then, let $\mu_N\left(t, \tau^{(j)}\right)$ refer to the resulting cumulated target state intensity of N, evaluated as

$$\begin{aligned} \mu_N\left(t, \tau^{(j)}\right) &= \left(\Lambda_N(t) + \int_0^{\tau^{(j)}} F_N(t_0)\mathcal{A}_N(t,s)dG_N(s)\right) \circ h_N(j) \circ D(B) \\ &+ \int_{\tau^{(j)}}^{t} (F_N(t_0)\mathcal{A}_N(t,s)dG_N(s)), \end{aligned} \tag{131}$$

where $\circ$ denotes element-wise product, $h_N(j)$ is a vector with indicators $h_{\langle xy\rangle}$ to identify the localized entangled connections of N that are entangled with qubit j, as

$$h_{\langle xy\rangle} = \begin{cases} 0, \text{if } x = j \\ 1, \text{otherwise} \end{cases}, \tag{132}$$

where $h_{\langle xy\rangle}$ is an indicator associated to $\langle xy\rangle$. Let $G_N(s, h(N))$ be defined as[148–150]

$$G_N(s, h(N)) = G_N^{t\leq\tau^{(j)}}(s, h(N)) + G_N^{t>\tau^{(j)}}(s, h(N)), \tag{133}$$

while $G_N^{t\leq\tau^{(j)}}(s, h(N))$ is an indicator for $t \leq \tau^{(j)}$ (i.e., $G_N^{t\leq\tau^{(j)}}(s, h(N))$ indicates the target state intensity before the localization in the intermediate node where the measurement is performed), while $G_N^{t>\tau^{(j)}}(s, h(N))$ is set for $t > \tau^{(j)}$ (i.e., $G_N^{t>\tau^{(j)}}(s, h(N))$ indicates the target state intensity after the localization onto the receiver node), and $D(B) = (B_1, \ldots, B_n)^T$ is a vector of n receivers for the localization procedure of target state intensity in the $\mathcal{L}_D$ downloading procedure, as

$$B_i = \begin{cases} 1, \text{if } j \in \mathcal{P}(A_i \rightarrow B_i) \\ 0, \text{otherwise} \end{cases}, \tag{134}$$

thus, if j belongs to the computational path $\mathcal{P}(A_i \rightarrow B_i)$ then B_i is a target node in $\mathcal{L}_D$.

As follows, the $\mu_N\left(t, \tau^{(j)}\right)$ cumulated target state intensity of the global entangled structure can be decomposed into a sum of target state intensities before measurement $M\left(\tau^{(j)}\right)[m_b]$ in the intermediate nodes, and after measurement in the target node. As a corollary of the $M\left(\tau^{(j)}\right)[m_b]$ measurement on j, for any $t \leq \tau^{(j)}$, the target state intensities of connections entangled with j vanish from the cumulated target state intensity in the intermediate nodes.

As the measurement on j is performed in the intermediate node, we focus to Bob B_i, to evaluate the target state intensity on his localized system state. As follows, at Bob B_i, the target state intensity of the localized system is as

$$\begin{aligned} \mu_{B_i}\left(t, \tau^{(j)}\right) &= \Lambda_{B_i}(t) + \int_0^{\tau^{(j)}} F_{B_i}(t_0)(t)\mathcal{A}_{B_i}(t,s)dG_{B_i}^{t>\tau^{(j)}}(s, h(N)) \\ &= F_{\langle jk\rangle}^{B_i}\left(t_0^{(j)}\right)e^{-\Delta_j\left(t-t_0^{(j)}\right)} + \sum_{l=1,l\neq k}^{\Gamma_j+1}\int_0^{\tau^{(j)}} F_{\langle jl\rangle}^{B_i}\left(t_0^{(l)}\right)e^{-\Delta_l(t-s)}dG_{B_i}^{t>\tau^{(j)}}(s, h(N)), \end{aligned} \tag{135}$$

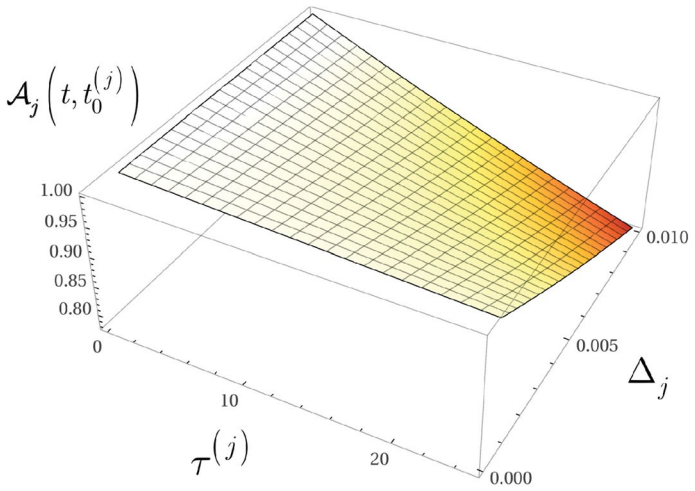

Figure 6. Scaling of the $\mathcal{A}_j\left(t, t_0^{(j)}\right)$ survival amplitude of the $\Lambda_{B_i}(t)$ target function intensity, $\Delta_j \in \left[10^{-3}, 10^{-2}\right]$, $\tau^{(j)} \in [0, 25], t_0^{(j)} = 0$.

where index B_i refers to the localized terms at Bob B_i.

The remaining, non-localized target function intensity belongs to the entangled connections in the intermediate network is evaluated as

$$\begin{aligned}\mu_N\left(\tau^{(j)}, t\right) =& \Lambda_N(t) + \int_0^{\tau^{(j)}} F_N(t_0)\mathcal{A}_N(t,s)dG_N^{t\leq\tau^{(j)}}(s, h(N)) \\ &+ \int_{\tau^{(j)}}^{t}\left(F_N(t_0)\mathcal{A}_N(t,s)dG_N^{t>\tau^{(j)}}(s, h(N))\right),\end{aligned} \tag{136}$$

therefore the target state intensities evolves further in the intermediate network, where the term $h_N(j)$ indicates that the entangled connections that affected by the measurement are vanished out from the cumulated intensity value.

Utilizing the framework of[148–150], (131) can be rewritten in a closed-form as

$$\begin{aligned}\mu_N\left(t, \tau^{(j)}\right) =& \left(\nu_{B_i}(t)\Lambda_{B_i}(t)\right) \\ &+ \left(\Lambda_N(t) + \zeta\left(t - \tau^{(j)}\right)F_N(t_0)\right)\left(h_N(j) \circ y\left(\tau^{(j)}\right)\right),\end{aligned} \tag{137}$$

where

$$\zeta\left(t - \tau^{(j)}\right) = e^{\left(F_N(t_0) - \Delta_N I\right)\left(t - \tau^{(j)}\right)}, \tag{138}$$

where Δ_N is a vector of decay rates of the entangled connections of N, $y\left(\tau^{(j)}\right)$ is

$$y\left(\tau^{(j)}\right) = \int_0^{\tau^{(j)}} e^{\Delta_N\left(\tau^{(j)} - s\right)} dG_N(s), \tag{139}$$

while $\nu_{B_i}(t)$ is a matrix function[148,149] associated to Bob's localized system, as

$$\begin{aligned}\nu_{B_i}(t) &= I + \int_0^{\tau^{(j)}} F_{B_i}(t_0)\mathcal{A}_{B_i}(t,s)\nu_{B_i}(s)ds \\ &= I + F_{B_i}(t_0)\left(F_{B_i}(t_0) - \Delta_{B_i}I\right)^{-1}\left(e^{\left(F_{B_i}(t_0) - \Delta_{B_i}I\right)t} - I\right),\end{aligned} \tag{140}$$

where Δ_{B_i} is a vector of decay rates of the localized entangled connections.

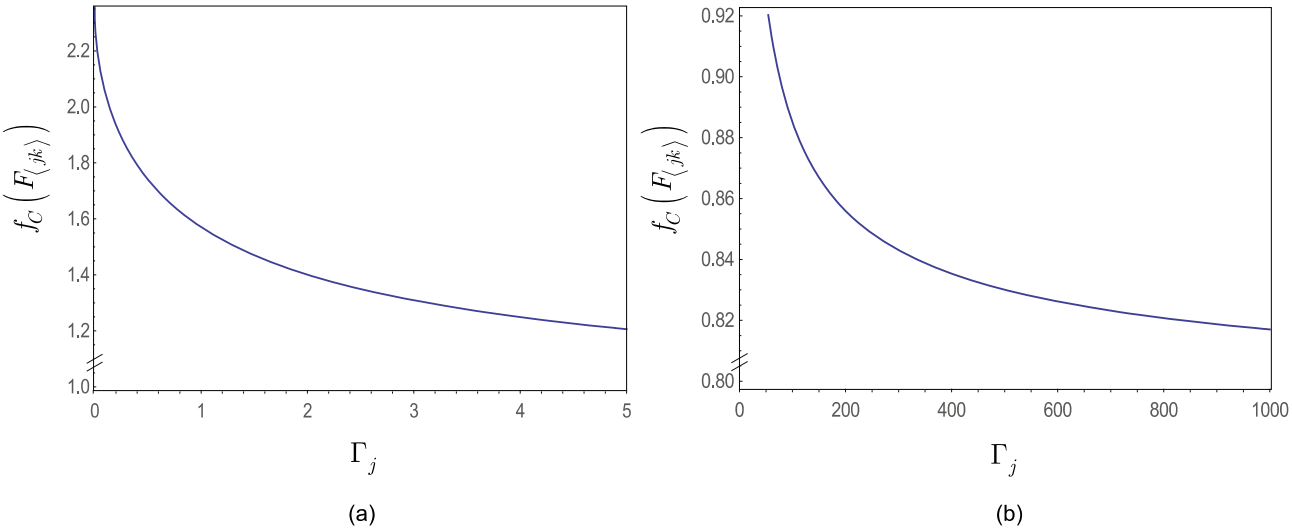

Figure 7. The cost function of $F_{\langle jk\rangle}$ scaled by (a) $\Gamma_j \in [0, 5]$, and (b) $\Gamma_j \in [0, 1000]$.

Since the target function values $F_{\langle jk\rangle}(t)$ are determined by $\left|\varphi^*_{N,jk}(t)\right\rangle$, it follows that at a target state decoherence the $F_{\langle jk\rangle}(t)$ target function values are therefore scalable via the $M[m_b]$ measurement associated to the localization procedure of the $\mathcal{L}_D$ downloading in the intermediate nodes.

The proof is concluded here. □

The scaled $\mathcal{A}_j\left(t, t_0^{(j)}\right)$ survival amplitude of the $\Lambda_{B_i}(t)$ target function intensity of a given $\langle jk\rangle$ at different $\tau^{(j)}$ measurement delays and Δ_j decay rates are depicted in Fig. 6.

Scaled computational cost. **Lemma 2** (Cost of target function evaluation). *The $f_C\left(F_{\langle jk\rangle}\right)$ computational cost associated to a given $F_{\langle jk\rangle}$ is the total application time of the local unitaries. The cost function is scalable via Γ_j in a multipartite entanglement system.*

Proof Let $\mathcal{P}(A \to B)$ be a computational path in N with L nodes and $(L-1)$ entangled connections. Then, for a given $\langle jk\rangle \in N$, let β_j^*, β_k^* and γ_{jk}^* refer to the gate parameters set to maximize the target function $F_{\langle jk\rangle}$, set via (109) and (110).

The $f_C\left(F_{\mathcal{P}(A\to B)}\right)$ computational cost of the maximization of target function $F_{\mathcal{P}(A\to B)}$ is defined as

$$f_C\left(F_{\mathcal{P}(A\to B)}\right) = \sum_{\langle jk\rangle \in \mathcal{P}(A\to B)} f_C\left(F_{\langle jk\rangle}\right), \tag{141}$$

where $f_C\left(F_{\langle jk\rangle}\right)$ is the computational cost associated to a given $F_{\langle jk\rangle}$ of an entangled connection $\langle jk\rangle$, as

$$f_C\left(F_{\langle jk\rangle}\right) = \beta_j^* + \beta_k^* + \gamma_{jk}^* = \tfrac{\pi}{4} + \tfrac{1}{2}\cos^{-1}\left(\tfrac{\Gamma_j - 1}{\Gamma_j + 1}\right). \tag{142}$$

that measures the computational cost as the total application time of the local unitaries.

As follows, (141) depends only on Γ_j, thus the scaling coefficient of the computational cost is Γ_j.

The $S_R\left(f_C\left(F_{\langle jk\rangle}\right)\right)$ series representation of (142) for $\left|\Gamma_j \Big/ \left(1+\Gamma_j\right)\right| < 1$, is

$$\begin{aligned} S_R\left(f_C\left(F_{\langle jk\rangle}\right)\right) &= \tfrac{1}{4}\left(2\cos^{-1}\left(\tfrac{\Gamma_j - 1}{\Gamma_j + 1}\right) + \pi\right) \\ &= \tfrac{3\pi}{4} - \sqrt{\tfrac{\Gamma_j}{\Gamma_j + 1}} \sum_{k=0}^{\infty} \frac{\left(\frac{1}{2}\right)\left(\frac{\Gamma_j}{\Gamma_j+1}\right)^k}{2k k! + k!}, \end{aligned} \tag{143}$$

while the $S_E\left(f_C\left(F_{\langle jk\rangle}\right)\right)$ series expansion of (142) at $\Gamma_j = \infty$ is as

$$\begin{aligned} S\left(f_C\left(F_{\langle jk\rangle}\right)\right) =& \tfrac{\pi}{4} + \sqrt{\tfrac{1}{\Gamma_j}} - \tfrac{1}{3}\left(\tfrac{1}{\Gamma_j}\right)^{3/2} + \tfrac{1}{5}\left(\tfrac{1}{\Gamma_j}\right)^{5/2} \\ & - \tfrac{1}{7}\left(\tfrac{1}{\Gamma_j}\right)^{7/2} + \tfrac{1}{9}\left(\tfrac{1}{\Gamma_j}\right)^{9/2} + \mathcal{O}\left(\left(\tfrac{1}{\Gamma_j}\right)^5\right). \end{aligned} \tag{144}$$

The $f_C(N)$ total computational cost of N at n computational paths, is therefore

$$f_C(N) = \sum_{q=1}^{n} f_C\left(F_{\mathcal{P}_q}\right) = \sum_{q=1}^{n} \sum_{\langle jk\rangle \in \mathcal{P}_q} f_C\left(F_{\langle jk\rangle}\right). \tag{145}$$

□

In Fig. 7, the scaled $f_C\left(F_{\langle jk\rangle}\right)$ cost function of $F_{\langle jk\rangle}$ is depicted.

Conclusions

Here, we defined a scalable model of distributed gate-model quantum computation in near-term quantum systems. We evaluated the scaling attributes and the unitaries of a distributed system for solving optimization problems. We showed that the computational model is an extended correlation space. We studied how decoherence affects the distributed computational model and characterized a cost function. The proposed results are applicable in different scenarios of experimental gate-model quantum computations.

Data availability

This work does not have any experimental data.

Received: 18 May 2020; Accepted: 30 October 2020
Published online: 26 February 2021

References

1. Preskill, J. Quantum computing in the NISQ era and beyond. *Quantum* **2**, 79 (2018).
2. Arute, F. *et al.* Quantum supremacy using a programmable superconducting processor. *Nature* https://doi.org/10.1038/s41586-019-1666-5 (2019).
3. Harrow, A. W. & Montanaro, A. Quantum computational supremacy. *Nature* **549**, 203–209 (2017).
4. Aaronson, S. & Chen, L. Complexity-theoretic foundations of quantum supremacy experiments. In *Proceedings of the 32nd Computational Complexity Conference, CCC'17*, 22:1–22:67 (2017).
5. Alexeev, Y. *et al.* Quantum Computer Systems for Scientific Discovery, arXiv:1912.07577 (2019).
6. Loncar, M. *et al.* Development of Quantum InterConnects for Next-Generation Information Technologies, arXiv:1912.06642 (2019).
7. Foxen, B. *et al.* Demonstrating a continuous set of two-qubit gates for near-term quantum algorithms. *Phys. Rev. Lett.* **125**, 120504 (2020).
8. Ajagekar, A., Humble, T. & You, F. Quantum computing based hybrid solution strategies for large-scale discrete-continuous optimization problems. *Comput. Chem. Eng.* **132**, 106630 (2020).
9. Ajagekar, A. & You, F. Quantum computing for energy systems optimization: challenges and opportunities. *Energy* **179**, 76–89 (2019).
10. Harrigan, M. *et al.* Quantum Approximate Optimization of Non-Planar Graph Problems on a Planar Superconducting Processor, arXiv:2004.04197v1 (2020).
11. Rubin, N. *et al.* Hartree–Fock on a superconducting qubit quantum computer. *Science* **369**(6507), 1084–1089 (2020).
12. Farhi, E., Goldstone, J. & Gutmann, S. A Quantum Approximate Optimization Algorithm, arXiv:1411.4028v1 (2014).
13. Farhi, E., Goldstone, J., Gutmann, S. & Zhou, L. The Quantum Approximate Optimization Algorithm and the Sherrington-Kirkpatrick Model at Infinite Size, arXiv:1910.08187 (2019).
14. Farhi, E., Goldstone, J., Gutmann, S. & Neven, H. Quantum Algorithms for Fixed Qubit Architectures. arXiv:1703.06199v1 (2017).
15. Sax, I. *et al.* Approximate approximation on a quantum annealer. In *Proceedings of the 17th ACM International Conference on Computing Frontiers (CF 2020)* (2020).
16. Brown, K. A. & Roser, T. Towards storage rings as quantum computers. *Phys. Rev. Accel. Beams* **23**, 054701 (2020).
17. Gyongyosi, L. Quantum state optimization and computational pathway evaluation for gate-model quantum computers. *Sci. Rep.* https://doi.org/10.1038/s41598-020-61316-4 (2020).
18. Gyongyosi, L. Unsupervised quantum gate control for gate-model quantum computers. *Sci. Rep.* https://doi.org/10.1038/s41598-020-67018-1 (2020).
19. Gyongyosi, L. & Imre, S. Circuit depth reduction for gate-model quantum computers. *Sci. Rep.* https://doi.org/10.1038/s41598-020-67014-5 (2020).
20. Gyongyosi, L. Objective function estimation for solving optimization problems in gate-model quantum computers. *Sci. Rep.* https://doi.org/10.1038/s41598-020-71007-9 (2020).
21. Gyongyosi, L. Decoherence dynamics estimation for superconducting gate-model quantum computers. *Quantum Inf. Process.* **19**, 369. https://doi.org/10.1007/s11128-020-02863-7 (2020).
22. Teplukhin, A., Kendrick, B. & Babikov, D. Solving complex eigenvalue problems on a quantum annealer with applications to quantum scattering resonances. *Phys. Chem. Chem. Phys.* https://doi.org/10.1039/D0CP04272B (2020).
23. Gill, S. S. *et al.Quantum Computing: A Taxonomy* (ACM Comput Surv, submitted, Systematic Review and Future Directions, 2020).
24. Xin, T. Improved Quantum State Tomography for Superconducting Quantum Computing Systems, arXiv:2006.15872v1 (2020).
25. Farhi, E., Kimmel, S. & Temme, K. A Quantum Version of Schoning's Algorithm Applied to Quantum 2-SAT, arXiv:1603.06985 (2016).
26. Farhi, E., Gamarnik, D. & Gutmann, S. The Quantum Approximate Optimization Algorithm Needs to See the Whole Graph: A Typical Case, arXiv:2004.09002v1 (2020).
27. Arute, F. *et al.* Observation of Separated Dynamics of Charge and Spin in the Fermi–Hubbard Model, arXiv:2010.07965 (2020).
28. Farhi, E., Gamarnik, D. & Gutmann, S. The Quantum Approximate Optimization Algorithm Needs to See the Whole Graph: Worst Case Examples, arXiv:arXiv:2005.08747 (2020).
29. Lloyd, S. Quantum Approximate Optimization is Computationally Universal, arXiv:1812.11075 (2018).
30. Pirandola, S. & Braunstein, S.L. Unite to build a quantum internet. *Nature* **532**, 169–171 (2016).
31. Pirandola, S. End-to-end capacities of a quantum communication network. *Commun. Phys.* **2**, 51 (2019).
32. Wehner, S., Elkouss, D. & Hanson, R. Quantum internet: a vision for the road ahead. *Science* **362**, 6412 (2018).
33. Pirandola, S., Laurenza, R., Ottaviani, C. & Banchi, L. Fundamental limits of repeaterless quantum communications. *Nat. Commun.* **8**, 15043. https://doi.org/10.1038/ncomms15043 (2017).

34. Pirandola, S. *et al.* Theory of channel simulation and bounds for private communication. *Quantum Sci. Technol.* **3**, 035009 (2018).
35. Pirandola, S. Bounds for multi-end communication over quantum networks. *Quantum Sci. Technol.* **4**, 045006 (2019).
36. Pirandola, S. Capacities of Repeater-assisted Quantum Communications, arXiv:1601.00966 (2016).
37. Pirandola, S. *et al.* Advances in quantum cryptography. *Adv. Opt. Photon.* https://doi.org/10.1364/AOP.361502 (2020).
38. Laurenza, R. & Pirandola, S. General bounds for sender-receiver capacities in multipoint quantum communications. *Phys. Rev. A* **96**, 032318 (2017).
39. Van Meter, R. *Quantum Networking*. ISBN 1118648927, 9781118648926 (Wiley, 2014).
40. Kimble, H. J. The quantum internet. *Nature* **453**, 1023–1030 (2008).
41. Gyongyosi, L. & Imre, S. Decentralized Base-Graph routing for the quantum internet. *Phys. Rev. A* https://doi.org/10.1103/PhysRevA.98.022310 (2018).
42. Gyongyosi, L. & Imre, S. Optimizing high-efficiency quantum memory with quantum machine learning for near-term quantum devices. *Sci. Rep.* https://doi.org/10.1038/s41598-019-56689-0 (2019).
43. Gyongyosi, L. & Imre, S. Theory of noise-scaled stability bounds and entanglement rate maximization in the quantum internet. *Sci. Rep.* https://doi.org/10.1038/s41598-020-58200-6 (2020).
44. Van Meter, R., Ladd, T. D., Munro, W. J. & Nemoto, K. System design for a long-line quantum repeater. *IEEE/ACM Trans. Netw.* **17**(3), 1002–1013 (2009).
45. Van Meter, R., Satoh, T., Ladd, T. D., Munro, W. J. & Nemoto, K. Path selection for quantum repeater networks. *Netw. Sci.* **3**(1–4), 82–95 (2013).
46. Van Meter, R. & Devitt, S. J. Local and distributed quantum computation. *IEEE Comput.* **49**(9), 31–42 (2016).
47. Gyongyosi, L. & Imre, S. Dynamic topology resilience for quantum networks. In *Proc. SPIE 10547, Advances in Photonics of Quantum Computing, Memory, and Communication XI*, 105470Z. https://doi.org/10.1117/12.2288707 (2018).
48. Gyongyosi, L. & Imre, S. Topology adaption for the quantum internet. *Quantum Inf. Process.* https://doi.org/10.1007/s11128-018-2064-x (2018).
49. Gyongyosi, L. & Imre, S. Entanglement access control for the quantum internet. *Quantum Inf. Process.* https://doi.org/10.1007/s11128-019-2226-5 (2019).
50. Gyongyosi, L. & Imre, S. Opportunistic entanglement distribution for the quantum internet. *Sci. Rep.* https://doi.org/10.1038/s41598-019-38495-w (2019).
51. Gyongyosi, L. & Imre, S. Adaptive routing for quantum memory failures in the quantum internet. *Quantum Inf. Process.* https://doi.org/10.1007/s11128-018-2153-x (2018).
52. Quantum Internet Research Group (QIRG). https://datatracker.ietf.org/rg/qirg/about/ (2018).
53. Gyongyosi, L. & Imre, S. Multilayer optimization for the quantum internet. *Sci. Rep.* https://doi.org/10.1038/s41598-018-30957-x (2018).
54. Gyongyosi, L. & Imre, S. Entanglement availability differentiation service for the quantum internet. *Sci. Rep.* https://doi.org/10.1038/s41598-018-28801-3 (2018).
55. Gyongyosi, L. & Imre, S. Entanglement-gradient routing for quantum networks. *Sci. Rep.* https://doi.org/10.1038/s41598-017-14394-w (2017).
56. Gyongyosi, L. & Imre, S. A survey on quantum computing technology. *Comput. Sci. Rev.* https://doi.org/10.1016/j.Cosrev.2018.11.002 (2018).
57. Rozpedek, F. *et al.* Optimizing practical entanglement distillation. *Phys. Rev. A* **97**, 062333 (2018).
58. Humphreys, P. *et al.* Deterministic delivery of remote entanglement on a quantum network. *Nature***558** (2018).
59. Liao, S.-K. *et al.* Satellite-to-ground quantum key distribution. *Nature* **549**, 43–47 (2017).
60. Ren, J.-G. *et al.* Ground-to-satellite quantum teleportation. *Nature* **549**, 70–73 (2017).
61. Hensen, B. et al., Loophole-free Bell inequality violation using electron spins separated by 1.3 kilometres. *Nature* 526 (2015).
62. Hucul, D. *et al.* Modular entanglement of atomic qubits using photons and phonons. *Nat. Phys.***11**(1) (2015).
63. Noelleke, C. *et al.* Efficient teleportation between remote single-atom quantum memories. *Phys. Rev. Lett.* **110**, 140403 (2013).
64. Sangouard, N. *et al.* Quantum repeaters based on atomic ensembles and linear optics. *Rev. Mod. Phys.* **83**, 33 (2011).
65. Caleffi, M. End-to-end entanglement rate: toward a quantum route metric. In *IEEE Globecom* (2017) https://doi.org/10.1109/GLOCOMW.2017.8269080(2018).
66. Caleffi, M. Optimal routing for quantum networks. *IEEE Access***5**. https://doi.org/10.1109/ACCESS.2017.2763325 (2017).
67. Caleffi, M., Cacciapuoti, A. S. & Bianchi, G. Quantum internet: from communication to distributed computing. In *NANOCOM'18: Proceedings of the 5th ACM International Conference on Nanoscale Computing and Communication* (2018).
68. Castelvecchi, D. The quantum internet has arrived. *Nature*. https://www.nature.com/articles/d41586-018-01835-3 (2018).
69. Cacciapuoti, A. S. *et al.* Quantum internet: networking challenges in distributed quantum computing. *IEEE Netw.* https://doi.org/10.1109/MNET.001.1900092 (2018).
70. Cuomo, D., Caleffi, M. & Cacciapuoti, A. S. Towards a distributed quantum computing ecosystem. https://digital-library.theiet.org/content/journals/10.1049/iet-qtc.2020.0002 (2020).
71. Chakraborty, K., Rozpedeky, F., Dahlbergz, A. & Wehner, S. Distributed Routing in a Quantum Internet. arXiv:1907.11630v1 (2019).
72. Khatri, S., Matyas, C. T., Siddiqui, A. U. & Dowling, J. P. Practical figures of merit and thresholds for entanglement distribution in quantum networks. *Phys. Rev. Res.* **1**, 023032 (2019).
73. Kozlowski, W. & Wehner, S. Towards large-scale quantum networks. In *Proc. of the Sixth Annual ACM International Conference on Nanoscale Computing and Communication*, Dublin, Ireland, (2019).
74. Pathumsoot, P. *et al.* Modeling of measurement-based quantum network coding on IBMQ devices. *Phys. Rev. A* **101**, 052301 (2020).
75. Pal, S., Batra, P., Paterek, T. & Mahesh, T. S. Experimental Localisation of Quantum Entanglement Through Monitored Classical Mediator. arXiv:1909.11030v1 (2019).
76. Miguel-Ramiro, J. & Dur, W. Delocalized information in quantum networks. *New J. Phys.* https://doi.org/10.1088/1367-2630/ab784d (2020).
77. Pirker, A. & Dur, W. A quantum network stack and protocols for reliable entanglement-based networks. *New J. Phys.* **21**, 033003. https://doi.org/10.1088/1367-2630/ab05f7 (2019).
78. Krisnanda, T. *et al.* Probing quantum features of photosynthetic organisms. *NPJ Quantum Inf.* **4**, 60 (2018).
79. Krisnanda, T. *et al.* Revealing nonclassicality of inaccessible objects. *Phys. Rev. Lett.* **119**, 120402 (2017).
80. Krisnanda, T. *et al.* Observable quantum entanglement due to gravity. *NPJ Quantum Inf.* **6**, 12 (2020).
81. Krisnanda, T. *et al.* Detecting nondecomposability of time evolution via extreme gain of correlations. *Phys. Rev. A* **98**, 052321 (2018).
82. Shannon, K., Towe, E. & Tonguz, O. On the Use of Quantum Entanglement in Secure Communications: A Survey, arXiv:2003.07907 (2020).
83. Amoretti, M. & Carretta, S. Entanglement verification in quantum networks with tampered nodes. *IEEE J. Sel. Areas Commun.* https://doi.org/10.1109/JSAC.2020.2967955 (2020).
84. Cao, Y. *et al.* Multi-tenant provisioning for quantum key distribution networks with heuristics and reinforcement learning: a comparative study. *IEEE Trans. Netw. Serv. Manag.* https://doi.org/10.1109/TNSM.2020.2964003 (2020).

85. Cao, Y. *et al.* Key as a service (KaaS) over quantum key distribution (QKD)-integrated optical networks. *IEEE Commun. Mag.* https://doi.org/10.1109/MCOM.2019.1701375 (2019).
86. Khatri, S. Policies for Elementary Link Generation in Quantum Networks, arXiv:2007.03193 (2020).
87. Miguel-Ramiro, J., Pirker, A. & Dur, W. Genuine Quantum Networks: Superposed Tasks and Addressing, arXiv:2005.00020v1 (2020).
88. Liu, Y. Preliminary Study of Connectivity for Quantum Key Distribution Network, arXiv:2004.11374v1 (2020).
89. Amer, O., Krawec, W. O. & Wang, B. Efficient Routing for Quantum Key Distribution Networks, arXiv:2005.12404 (2020).
90. Sun, F. Performance analysis of quantum channels. *Quantum Eng.* https://doi.org/10.1002/que2.35 (2020).
91. Chai, G. *et al.* Blind channel estimation for continuous-variable quantum key distribution. *Quantum Eng.* https://doi.org/10.1002/que2.37 (2020).
92. Ahmadzadegan, A. *et al.* Learning to Utilize Correlated Auxiliary Classical or Quantum Noise, arXiv:2006.04863v1 (2020).
93. Bausch, J. Recurrent quantum neural networks. In *Advances in Neural Information Processing Systems (NeurIPS 2020)* 33 (2020).
94. Dong, K. *et al.* Distributed subkey-relay-tree-based secure multicast scheme in quantum data center networks. *Opt. Eng.* **59**(6), 065102. https://doi.org/10.1117/1.OE.59.6.065102 (2020).
95. Mewes, L. *et al.* Energy relaxation pathways between light-matter states revealed by coherent two-dimensional spectroscopy. *Commun. Phys.* **3**, 157 (2020).
96. Kopszak, P., Mozrzymas, M. & Studzinski, M. Positive maps from irreducibly covariant operators. *J. Phys. A Math. Theor.* **53**, 395306 (2020).
97. Guo, D. *et al.* Comprehensive high-speed reconciliation for continuous-variable quantum key distribution. *Quantum Inf. Process.* **19**, 320 (2020).
98. Chen, L. & Hu, M. Locally maximally mixed states. *Quantum Inf. Process.* **19**, 305 (2020).
99. Barbeau, M. *et al.* Capacity requirements in networks of quantum repeaters and terminals. In: *Proc. of IEEE Int. Conf. on Quantum Computing and Engineering (QCE 2020)* (2020).
100. Yin, J. *et al.* Entanglement-based secure quantum cryptography over 1,120 kilometres. *Nature* **582**, 501 (2020).
101. Santra, S. & Malinovsky, V. S. Quantum Networking with Short-Range Entanglement Assistance, arXiv:2008.05553 (2020).
102. Komarova, K. *et al.* Quantum device emulates dynamics of two coupled oscillators. *J. Phys. Chem. Lett.* https://doi.org/10.1021/acs.jpclett.0c01880 (2020).
103. Gattuso, H. *et al.* Massively parallel classical logic via coherent dynamics of an ensemble of quantum systems with dispersion in size. *ChemRxiv* https://doi.org/10.26434/chemrxiv.12370538.v1 (2020).
104. Chessa, S., Giovannetti, V. Multi-Level Amplitude Damping Channels: Quantum Capacity Analysis, arXiv:2008.00477 (2020).
105. Pozzi, M. G. *et al.* Using Reinforcement Learning to Perform Qubit Routing in Quantum Compilers, arXiv:2007.15957 (2020).
106. Bartkiewicz, K. *et al.* Experimental kernel-based quantum machine learning in finite feature space. *Sci. Rep.* **10**, 12356. https://doi.org/10.1038/s41598-020-68911-5 (2020).
107. Kozlowski, W., Dahlberg, A. & Wehner, S. Designing a Quantum Network Protocol, arXiv:2010.02575 (2020).
108. Khan, T. M. & Robles-Kelly, A. A derivative-free method for quantum perceptron training in multi-layered neural networks. In *ICONIP 2020* (2020).
109. Mehic, M. *et al.* Quantum key distribution: a networking perspective. *ACM Comput. Surv.* https://doi.org/10.1145/3402192 (2020).
110. Kao, J. & Chou, C. Entangling capacities and the geometry of quantum operations. *Sci. Rep.* **10**, 15978. https://doi.org/10.1038/s41598-020-72881-z (2020).
111. Bae, J. *et al.* Quantum circuit optimization using quantum Karnaugh map. *Sci. Rep.* **10**, 15651. https://doi.org/10.1038/s41598-020-72469-7 (2020).
112. Bugu, S., Ozaydin, F. & Kodera, T. Surpassing the Classical Limit in Magic Square Game with Distant Quantum Dots Coupled to Optical Cavities, arXiv:2011.01490 (2020).
113. Welland, I. & Ferry, D. K. Wavepacket phase-space quantum Monte Carlo method. *J. Comput. Electron.* https://doi.org/10.1007/s10825-020-01602-6 (2020).
114. Ferguson, M. S., Zilberberg, O. & Blatter, G. Open Quantum Systems Beyond Fermi's Golden Rule: Diagrammatic Expansion of the Steady-State Time-Convolutionless Master Equation, arXiv:2010.09838 (2020).
115. Villalba-Diez, J. & Zheng, X. Quantum strategic organizational design: alignment in industry 4.0 complex-networked cyber-physical lean management systems. *Sensors* **20**, 5856. https://doi.org/10.3390/s20205856 (2020).
116. Krisnanda, T. Distribution of quantum entanglement: Principles and applications, PhD Dissertation, Nanyang Technological University, arXiv:2003.08657 (2020).
117. Ghosh, S. *et al.* Universal quantum reservoir computing. arXiv:2003.09569 (2020).
118. Gyongyosi, L. Dynamics of entangled networks of the quantum internet. *Sci. Rep.* https://doi.org/10.1038/s41598-020-68498-x (2020).
119. Gyongyosi, L. & Imre, S. Routing space exploration for scalable routing in the quantum internet. *Sci. Rep.* https://doi.org/10.1038/s41598-020-68354-y (2020).
120. Lloyd, S. & Weedbrook, C. Quantum generative adversarial learning. *Phys. Rev. Lett.***121**, (2018).
121. Gisin, N. & Thew, R. Quantum communication. *Nat. Photon.* **1**, 165–171 (2007).
122. Xiao, Y. F. & Gong, Q. Optical microcavity: from fundamental physics to functional photonics devices. *Sci. Bull.* **61**, 185–186 (2016).
123. Zhang, W. *et al.* Quantum secure direct communication with quantum memory. *Phys. Rev. Lett.* **118**, 220501 (2017).
124. Enk, S. J., Cirac, J. I. & Zoller, P. Photonic channels for quantum communication. *Science* **279**, 205–208 (1998).
125. Briegel, H. J., Dur, W., Cirac, J. I. & Zoller, P. Quantum repeaters: the role of imperfect local operations in quantum communication. *Phys. Rev. Lett.* **81**, 5932–5935 (1998).
126. Dur, W., Briegel, H. J., Cirac, J. I. & Zoller, P. Quantum repeaters based on entanglement purification. *Phys. Rev. A* **59**, 169–181 (1999).
127. Duan, L. M., Lukin, M. D., Cirac, J. I. & Zoller, P. Long-distance quantum communication with atomic ensembles and linear optics. *Nature* **414**, 413–418 (2001).
128. Van Loock, P. *et al.* Hybrid quantum repeater using bright coherent light. *Phys. Rev. Lett.* **96**, 240501 (2006).
129. Zhao, B., Chen, Z. B., Chen, Y. A., Schmiedmayer, J. & Pan, J. W. Robust creation of entanglement between remote memory qubits. *Phys. Rev. Lett.* **98**, 240502 (2007).
130. Goebel, A. M. *et al.* Multistage entanglement swapping. *Phys. Rev. Lett.* **101**, 080403 (2008).
131. Simon, C. *et al.* Quantum repeaters with photon pair sources and multimode memories. *Phys. Rev. Lett.* **98**, 190503 (2007).
132. Tittel, W. *et al.* Photon-echo quantum memory in solid state systems. *Laser Photon. Rev.* **4**, 244–267 (2009).
133. Sangouard, N., Dubessy, R. & Simon, C. Quantum repeaters based on single trapped ions. *Phys. Rev. A* **79**, 042340 (2009).
134. Dur, W. & Briegel, H. J. Entanglement purification and quantum error correction. *Rep. Prog. Phys.* **70**, 1381–1424 (2007).
135. Sheng, Y. B. & Zhou, L. Distributed secure quantum machine learning. *Sci. Bull.* **62**, 1025–1029 (2017).
136. Leung, D., Oppenheim, J. & Winter, A. *IEEE Trans. Inf. Theory* **56**, 3478–90 (2010).
137. Kobayashi, H., Le Gall, F., Nishimura, H. & Rotteler, M. Perfect quantum network communication protocol based on classical network coding. In *Proceedings of 2010 IEEE International Symposium on Information Theory (ISIT)*, 2686–90 (2010).

138. Gyongyosi, L. & Imre, S. Training optimization for gate-model quantum neural networks. *Sci. Rep.* https://doi.org/10.1038/s41598-019-48892-w (2019).
139. Gyongyosi, L. & Imre, S. Dense quantum measurement theory. *Sci. Rep.* https://doi.org/10.1038/s41598-019-43250-2 (2019).
140. Gyongyosi, L. & Imre, S. State stabilization for gate-model quantum computers. *Quantum Inf. Process.* https://doi.org/10.1007/s11128-019-2397-0 (2019).
141. Gyongyosi, L. & Imre, S. Quantum circuit design for objective function maximization in gate-model quantum computers. *Quantum Inf. Process.* https://doi.org/10.1007/s11128-019-2326-2 (2019).
142. Morimae, T. How to upload a physical state to the correlation space. *Phys. Rev. A* **83**, 042337 (2011).
143. Cai, J.-M. *et al.* Quantum computation in correlation space and extremal entanglement. *Phys. Rev. Lett.* **103**, 050503 (2009).
144. Gross, D. & Eisert, J. Novel schemes for measurement-based quantum computation. *Phys. Rev. Lett.* **98**, 220503 (2007).
145. Gross, D. & Eisert, J. Quantum computational webs. *Phys. Rev. A* **82**, 040303 (2010).
146. Beau, M., Kiukas, J., Egusquiza, I. L. & del Campo, A. Nonexponential quantum decay under systemal decoherence. *Phys. Rev. Lett.* **119**, 130401 (2017).
147. Fonda, L., Ghirardi, G. C. & Rimini, A. *Rep. Prog. Phys.* **41**, 587 (1978).
148. Gupta, A. *et al.* Discrete interventions in hawkes processes with applications in invasive species management. In *Proceedings of the 27th International Joint Conference on Artificial Intelligence (IJCAI-18)* (2018).
149. Farajtabar, M. *et al.* Shaping social activity by incentivizing users. In *NIPS*, 2474–2482, (2014).
150. Farajtabar, M. *et al. Multistage campaigning in social networks, NIPS*, 4718–4726 (2016).
151. Farhi, E. & Neven, H. Classification with Quantum Neural Networks on Near Term Processors, arXiv:1802.06002v1 (2018).
152. Lloyd, S. *et al.* Infrastructure for the quantum internet. *ACM SIGCOMM Comput. Commun. Rev.* **34**, 9–20 (2004).
153. Gyongyosi, L., Imre, S. & Nguyen, H. V. A survey on quantum channel capacities. *IEEE Commun. Surv. Tutor.* https://doi.org/10.1109/COMST.2017.2786748 (2018).
154. Gyongyosi, L., Bacsardi, L. & Imre, S. A survey on quantum key distribution. *Infocom. J XI* **2**, 14–21 (2019).
155. Imre, S. & Gyongyosi, L. *Advanced Quantum Communications—An Engineering Approach* (Wiley-IEEE Press, New Jersey, 2013).
156. Kok, P. *et al.* Linear optical quantum computing with photonic qubits. *Rev. Mod. Phys.* **79**, 135–174 (2007).
157. Petz, D. *Quantum Information Theory and Quantum Statistics* (Springer, Heidelberg, 2008).
158. Bacsardi, L. On the way to quantum-based satellite communication. *IEEE Commun. Mag.* **51**(08), 50–55 (2013).
159. Biamonte, J. *et al.* Quantum machine learning. *Nature* **549**, 195–202 (2017).
160. Lloyd, S., Mohseni, M. & Rebentrost, P. Quantum Algorithms for Supervised and Unsupervised Machine Learning. arXiv:1307.0411 (2013).
161. Lloyd, S., Mohseni, M. & Rebentrost, P. Quantum principal component analysis. *Nat. Phys.* **10**, 631 (2014).
162. Lloyd, S. Capacity of the noisy quantum channel. *Phys. Rev. A* **55**, 1613–1622 (1997).
163. Lloyd, S. The Universe as Quantum Computer, *A Computable Universe: Understanding and exploring Nature as computation*, Zenil, H. ed., World Scientific, Singapore. arXiv:1312.4455v1 (2013).
164. Shor, P. W. Scheme for reducing decoherence in quantum computer memory. *Phys. Rev. A* **52**, R2493–R2496 (1995).
165. Chou, C. *et al.* Functional quantum nodes for entanglement distribution over scalable quantum networks. *Science* **316**(5829), 1316–1320 (2007).
166. Muralidharan, S., Kim, J., Lutkenhaus, N., Lukin, M. D. & Jiang, L. Ultrafast and fault-tolerant quantum communication across long distances. *Phys. Rev. Lett.* **112**, 250501 (2014).
167. Yuan, Z. *et al. Nature* **454**, 1098–1101 (2008).
168. Kobayashi, H., Le Gall, F., Nishimura, H. & Rotteler, M. General scheme for perfect quantum network coding with free classical communication. In *Lecture Notes in Computer Science* (Automata, Languages and Programming SE-52 vol. 5555), 622–633 (Springer, 2009).
169. Hayashi, M. Prior entanglement between senders enables perfect quantum network coding with modification. *Phys. Rev. A* **76**, 040301(R) (2007).
170. Hayashi, M., Iwama, K., Nishimura, H., Raymond, R. & Yamashita, S. Quantum network coding. In *Lecture Notes in Computer Science (STACS 2007 SE52 vol. 4393)* (eds Thomas, W. & Weil, P.) (Springer, Berlin, 2007).
171. Chen, L. & Hayashi, M. Multicopy and stochastic transformation of multipartite pure states. *Phys. Rev. A* **83**(2), 022331 (2011).
172. Schoute, E., Mancinska, L., Islam, T., Kerenidis, I. & Wehner, S. Shortcuts to quantum network routing, arXiv:1610.05238 (2016).
173. Azuma, K., Tamaki, K. & Lo, H.-K. All-photonic quantum repeaters. *Nat. Commun.* **6**, 6787 (2015).

Acknowledgements

The research reported in this paper has been supported by the Hungarian Academy of Sciences (MTA Premium Postdoctoral Research Program 2019), by the National Research, Development and Innovation Fund (TUDFO/51757/2019-ITM, Thematic Excellence Program), by the National Research Development and Innovation Office of Hungary (Project No. 2017-1.2.1-NKP-2017-00001), by the Hungarian Scientific Research Fund—OTKA K-112125 and in part by the BME Artificial Intelligence FIKP grant of EMMI (Budapest University of Technology, BME FIKP-MI/SC), and by the Ministry of Innovation and Technology and the National Research, Development and Innovation Office within the Quantum Information National Laboratory of Hungary.

Author contributions

L.GY. designed the protocol and wrote the manuscript. L.GY. and S.I. and analyzed the results.

Funding

No relevant funding.

Competing interests

The authors declare that no competing interests.

Additional information

Supplementary Information The online version contains supplementary material available at https://doi.org/10.1038/s41598-020-76728-5.

Correspondence and requests for materials should be addressed to L.G.

Reprints and permissions information is available at www.nature.com/reprints.